MAR 29 1932

Library L.M.A.L.

TECHNICAL NOTES

NATIONAL ADVISORY COMMITTEE FOR AERONAUTICS

3 1176 00080 7124

No. 412

THE AERODYNAMIC CHARACTERISTICS OF AIRFOILS AT NEGATIVE ANGLES OF ATTACK

By Raymond F. Anderson
Langley Memorial Aeronautical Laboratory

FILE COPY
To be returned to
the files of the Langley
Memorial Aeronautical
Laboratory

Washington
March, 1932

E R R A T A

NATIONAL ADVISORY COMMITTEE FOR AERONAUTICS

TECHNICAL NOTE NO. 412

THE AERODYNAMIC CHARACTERISTICS OF AIRFOILS AT NEGATIVE ANGLES OF ATTACK

Figure 10: The c.p. at -7.9° should be 14.9 per cent instead of 4.9 per cent.

Figure 20: The part of the c.p. curve from -14° extending to and beyond -8° should be concave upwards. The true form of these and other c.p. curves may be obtained more accurately by computing c.p. values from the curves of $C_{m\ c/4}$.

NATIONAL ADVISORY COMMITTEE FOR AERONAUTICS

TECHNICAL NOTE NO. 412

THE AERODYNAMIC CHARACTERISTICS OF AIRFOILS AT NEGATIVE ANGLES OF ATTACK

By Raymond F. Anderson

SUMMARY

A number of airfoils, including 14 commonly used airfoils and 10 N.A.C.A. airfoils, were tested through the negative angle-of-attack range in the N.A.C.A. variable-density wind tunnel at a Reynolds Number of approximately 3,000,000. The tests were made to supply data to serve as a basis for the structural design of airplanes in the inverted flight condition. In order to make the results immediately available for this purpose they are presented herein in preliminary form, together with results of previous tests of the airfoils at positive angles of attack.

An analysis of the results made to find the variation of the ratio of the maximum negative lift coefficient to the maximum positive lift coefficient led to the following conclusions:

1. For airfoils of a given thickness, the ratio $-C_{L\ max}/+C_{L\ max}$ tends to decrease as the mean camber is increased.

2. For airfoils of a given mean camber, the ratio $-C_{L\ max}/+C_{L\ max}$ tends to increase as the thickness increases.

INTRODUCTION

There is at present little information on the aerodynamic characteristics of airfoils at negative angles of attack. In the few tests which have been made the Reynolds Number has been low.

The need for additional data in this range was recently experienced by the Bureau of Aeronautics, Navy Department, while they were formulating rational procedures to be followed in designing airplanes for the dive and inverted flight conditions. Accordingly, a number of airfoils suggested by the Bureau of Aeronautics and a number of N.A.C.A. airfoils were tested at negative angles of attack in the N.A.C.A. variable-density wind tunnel at a Reynolds Number of approximately 3,000,000.

Part of the results were published in a preliminary note (reference 1) before the tests were completed. The present report gives all the results, including those published in reference 1 and the results of previously unpublished tests of the airfoils at positive angles of attack.

APPARATUS AND METHOD

A brief description of the redesigned variable-density wind tunnel and its method of operation will be found in reference 2. The customary 5 by 30 inch polished duralumin airfoils were used in the tests. In reference 2 will be found a description of the method of constructing the airfoils. The specified ordinates will be found in Table I.

The airfoils were tested in the usual manner (as described in reference 2) except for the method of mounting on the support struts. When airfoils are tested at positive angles of attack they are mounted on the support struts of the balance with the sting and struts attached on the flat side. For these tests, however, the airfoils were inverted and the sting was placed on the curved surface to leave the flat surface free from obstructions that might affect the value of the maximum negative lift coefficient.

The measurements of lift, drag, and pitching moment were made at a pressure of approximately 20 atmospheres and an air speed of approximately 70 feet per second, which correspond to a Reynolds Number of 3,100,000. The tests at positive angles of attack were made under the same conditions.

ACCURACY

After the tests were completed, check tests were made on some of the N.A.C.A. airfoils. The maximum lift coefficients were found to be of the order of 3 per cent lower than the values obtained in the first tests. It was suspected that the difference might have been due to roughening of the noses of the airfoils by particles in the air stream. Several of the N.A.C.A. airfoils were therefore repolished on the nose and on retest gave values of maximum lift coefficients approximately equal to those obtained in the first tests. It was therefore apparent that in order to make accurate comparison of the maximum lift coefficients possible, special care was necessary in finishing the noses of the airfoils. The differences between the surfaces of the airfoils used in the tests described in this report are not known, but it is estimated that the uncertainty in the maximum lift coefficients resulting from possible variations of the surface texture does not exceed ±3 per cent. Inasmuch as other sources of error may amount to ±1 per cent, the values of the maximum lift coefficients may be considered accurate to within ±4 per cent.

If the results of the present tests for the Clark Y, the M-6, the U.S.A. 27, and the U.S.A. 35B airfoils are compared with the results for these airfoils from the tests made in the original tunnel, the maximum lift coefficients from the earlier tests will be found to be lower. (Reference 3.) Although the original tunnel differed in some respects from the present one, most of the difference between the maximum lift coefficients is attributed to the use of unpolished airfoils in the original tunnel.

RESULTS AND DISCUSSION

The method used in obtaining the final results, including the correction for the influence of the tunnel walls, is given in reference 3. Values of C_L, C_D, C_{D_o}, $C_{m_{c/4}}$, and c.p. are plotted against angle of attack in Figures 1 to 24. These curves, together with the indicated values of C_{m_o} ($C_{m_{c/4}}$ when $C_L = 0$), present the data in preliminary form with sufficient accuracy for use in

structural design. A technical report will be published later which will give these and other results in a more complete form, including tables of the data.

To indicate the scale effect on the negative range of the lift curve, data on the CYH airfoil are compared in Figure 25. The curve from the test at low Reynolds Number shows a burble at a comparatively low angle of attack followed by a gradual increase in lift.

An effort has been made to find the variation of the maximum negative lift coefficients of these airfoils with the shapes of the profiles. For this purpose the ratio $\frac{-C_{L\ max}}{+C_{L\ max}}$ has been used. The determination of the variation of this ratio with the shape of the profile is difficult because of the large number of variables which determine the shape. However, a reasonably consistent variation of the ratio $\frac{-C_{L\ max}}{+C_{L\ max}}$ has been found with two shape characteristics of the profiles - the thickness (maximum) and the mean camber.

For the purpose of this analysis the mean camber is defined as the maximum departure of the mean line of the profile from the chord, where the chord is taken as the line joining the extremities of the mean line. The mean line is defined as a line midway between the upper and lower surfaces of the profile, where the thickness is measured perpendicular to the mean line.

In Figure 26 $\frac{-C_{L\ max}}{+C_{L\ max}}$ has been plotted against the mean camber and a line has been drawn in to represent the variation of $\frac{-C_{L\ max}}{+C_{L\ max}}$ with the mean camber for profiles of 12 per cent thickness. The values for profiles of approximately 12 per cent thickness lie near this line; whereas the values for thicker and thinner profiles lie above and below it, respectively. The ratios for the 2512, the 4512, and the 6512 (which have the mean camber at 0.5 of the chord and a thickness of 12 per cent) have the same trend as the general trend of the ratios; that is, $\frac{-C_{L\ max}}{+C_{L\ max}}$ decreases as the mean camber increases. The Clark Y, the Clark Y M-15, and the

Clark Y M-18 profiles, which have approximately the same mean camber, show an increase of $\frac{-C_{L\ max}}{+C_{L\ max}}$ as the thickness is increased. (The designation M means that the profiles were thickened from the mean ordinates of the original Clark Y.)

The plot may be used for making an estimate of the value of $-C_{L\ max}$ for any airfoil for which data are available from a variable-density tunnel test at positive angles of attack. The airfoil should be located on the plot according to its mean camber (found as described above) and thickness. If the airfoil is similar to one of those on the plot, the locating of it will be easier.

The error in the estimate is likely to be large if the profile has peculiarities of shape such as a sharp curvature of the leading or trailing sections, but for profiles of conventional shape, the error in the estimate of $-C_{L\ max}$ should not exceed 12 per cent of the true value.

CONCLUSIONS

1. For airfoils of a given thickness, the ratio $\frac{-C_{L\ max}}{+C_{L\ max}}$ tends to decrease as the mean camber is increased.

2. For airfoils of a given mean camber, the ratio $\frac{-C_{L\ max}}{+C_{L\ max}}$ tends to increase as the thickness is increased.

Langley Memorial Aeronautical Laboratory,
National Advisory Committee for Aeronautics,
Langley Field, Va., February 26, 1932.

REFERENCES

1. Anderson, Raymond F.: The Aerodynamic Characteristics of Six Commonly Used Airfoils over a Large Range of Positive and Negative Angles of Attack. T.N. No. 397, N.A.C.A., 1931.

2. Jacobs, Eastman N.: Tests of Six Symmetrical Airfoils in the Variable-Density Wind Tunnel. T.N. No. 385, N.A.C.A., 1931.

3. Jacobs, Eastman N., and Anderson, Raymond F.: Large Scale Aerodynamic Characteristics of Airfoils as Tested in the Variable-Density Wind Tunnel. T.R. No. 352, N.A.C.A., 1930.

4. Clark, K. W., and Lockspeiser, B.: Wind Tunnel Tests on Aerofoils at Negative Incidences. R. & M. No. 1383, British A.R.C., 1930.

TABLE I

Ordinates of the Airfoils in Per Cent of the Chord

Airfoil	Clark Y		Clark Y-18		Clark Y M-15		Clark Y M-18		U.S.A. 27	
L.E. Radius	1.50		----		----		----		----	
Stations	Upper	Lower	Upper	Lower	Upper	Lower	Upper	Lower	Upper	Lower
0	3.50	3.50	5.38	5.38	3.50	3.50	3.50	3.50	1.77	1.77
1-1/4	5.45	1.93	8.38	2.97	5.95	1.43	6.40	.98	3.80	.50
2-1/2	6.50	1.47	10.00	2.26	7.21	.76	7.85	.11	5.07	.36
5	7.90	.93	12.15	1.43	8.88	- .05	9.78	- .94	6.94	.19
7-1/2	8.85	.63	13.61	.97	10.01	- .53	11.06	-1.58	8.22	.10
10	9.60	.42	14.76	.65	10.89	- .87	12.07	-2.05	9.19	.02
15	10.68	.15	16.45	.23	12.17	-1.34	13.52	-2.69	10.50	.10
20	11.36	.03	17.47	.05	12.96	-1.56	14.41	-3.02	11.37	.36
30	11.70	0	18.00	0	13.35	-1.65	14.85	-3.15	11.97	.93
40	11.40	0	17.53	0	13.01	-1.61	14.47	-3.07	11.68	1.14
50	10.52	0	16.19	0	12.00	-1.48	13.35	-2.83	10.86	.75
60	9.15	0	14.07	0	10.44	-1.29	11.61	-2.46	9.54	.28
70	7.35	0	11.30	0	8.39	-1.04	9.33	-1.98	8.08	.06
80	5.22	0	8.03	0	5.95	- .74	6.62	-1.40	6.10	.01
90	2.80	0	4.31	0	3.20	- .40	3.56	- .75	3.69	.12
95	1.49	0	2.29	0	1.70	- .21	1.90	- .40	2.26	.33
100	.12	0	.18	0	.14	- .02	.15	- .03	.67	.65

TABLE I - CONTINUED

Ordinates of the Airfoils in Per Cent of the Chord - Continued

Airfoil	U.S.A. 35B		Boeing 103		Boeing 103A		NACA M6		NACA CYH	
L.E. Radius	---		1.25		0.97		---		1.50	
Stations	Upper	Lower	Upper	Lower	Upper	Lower	Upper	Lower	Upper	Lower
0	2.76	2.76	3.56	3.56	2.92	2.92	0	0	3.50	3.50
1-1/4	5.15	1.03	6.10	2.20	5.00	1.80	1.97	-1.76	5.45	1.93
2-1/2	6.11	.63	7.17	1.73	5.87	1.42	2.81	-2.20	6.50	1.47
5	7.52	.28	8.56	1.22	7.01	1.00	4.03	-2.73	7.90	.93
7-1/2	8.65	.14	9.55	.88	7.82	.72	4.94	-3.03	8.85	.63
10	9.45	.07	10.35	.64	8.48	.52	5.71	-3.24	9.60	.42
15	10.56	.00	11.53	.32	9.44	.26	6.82	-3.47	10.68	.15
20	11.28	.05	12.28	.15	10.00	.12	7.55	-3.62	11.36	.03
25							8.01	-3.71		
30	11.76	.15	12.70	.02	10.40	.02	8.22	-3.79	11.70	0
40	11.42	.28	12.42	0	10.17	0	8.05	-3.90	11.40	0
50	10.33	.39	11.56	.02	9.47	.02	7.26	-3.94	10.52	0
60	8.81	.45	10.21	.11	8.36	.08	6.03	-3.82	9.15	0
65									8.30	0
70	7.08	.42	8.38	.25	6.86	.17	4.58	-3.48	7.41	.06
80	5.02	.35	6.26	.46	5.13	.30	3.06	-2.83	5.62	.38
90	2.72	.20	3.84	.71	3.18	.45	1.55	-1.77	3.84	1.02
95	1.50	.12	2.50	.85	2.14	.53	.88	-1.08	2.93	1.40
100	.25	.00	1.11	1.00	.87	.87	.26	- .26	2.05	1.85
T.E. Radius	---		0.05		0.25		---		---	

TABLE I - CONTINUED

Ordinates of the Airfoils in Per Cent of the Chord - Continued

Airfoil	N 22		C 72		Boeing 106		Gött. 398	
L.E. Radius	---		1.40		0.70		---	
Stations	Upper	Lower	Upper	Lower	Upper	Lower	Upper	Lower
0	3.37	3.37	3.49	3.49	2.98	2.98	3.74	3.74
1-1/4	5.58	1.70	5.55	1.92	5.26	1.54	6.20	1.89
2-1/2	6.66	1.15	6.51	1.47	6.14	1.04	7.40	1.28
5	8.25	.62	7.89	.93	7.54	.42	9.17	.69
7-1/2	9.33	.32	8.85	.64	8.56	.04	10.37	.35
10	10.13	.16	9.60	.43	9.44	- .28	11.25	.18
15	11.28	.03	10.69	.16	10.62	- .64	12.53	.03
20	12.01	0	11.36	.03	11.34	- .90	13.34	0
30	12.42	.05	11.73	0	11.88	-1.18	13.80	.05
40	12.01	.15	11.41	.21	11.54	-1.28	13.34	.17
50	11.04	.24	10.53	.59	10.54	-1.30	12.27	.27
60	9.57	.30	9.15	.85	9.08	-1.22	10.63	.33
70	7.68	.32	7.36	.91	7.18	- .98	8.53	.35
80	5.51	.24	5.23	.72	4.96	- .72	6.12	.27
90	3.06	.12	2.80	.40	2.54	- .42	3.40	.13
95	1.73	.05	1.52	.21	1.29	- .23	1.92	.06
100	.40	0	.10	0	.04	- .04	.40	0

TABLE I - CONTINUED

Ordinates of the Airfoils in Per Cent of the Chord - Continued

Airfoil	NACA 2409		NACA 2412		NACA 2415		NACA 4412		NACA 2212	
L.E. Radius	0.887		1.576		2.464		1.576		1.576	
Slope of radius passing through end of chord	2/20		2/20		2/20		4/20		2/10	
Stations	Upper	Lower	Upper	Lower	Upper	Lower	Upper	Lower	Upper	Lower
0	-	0.00	-	0.00	-	0.00	-	0.00	-	0.00
1-1/4	1.62	-1.23	2.15	-1.65	2.71	-2.06	2.44	-1.43	2.44	-1.46
2-1/2	2.27	-1.66	2.99	-2.27	3.71	-2.86	3.39	-1.95	3.35	-1.96
5	3.20	-2.15	4.13	-3.01	5.07	-3.84	4.73	-2.49	4.62	-2.55
7-1/2	3.87	-2.44	4.96	-3.46	6.06	-4.47	5.76	-2.74	5.55	-2.89
10	4.43	-2.60	5.63	-3.75	6.83	-4.90	6.59	-2.86	6.27	-3.11
15	5.25	-2.77	6.61	-4.10	7.97	-5.42	7.89	-2.88	7.25	-3.44
20	5.81	-2.79	7.26	-4.23	8.70	-5.66	8.80	-2.74	7.74	-3.74
25	6.18	-2.74	7.67	-4.22	9.17	-5.70	9.41	-2.50	7.93	-3.94
30	6.38	-2.62	7.88	-4.12	9.38	-5.62	9.76	-2.26	7.97	-4.03
40	6.35	-2.35	7.80	-3.80	9.25	-5.25	9.80	-1.80	7.68	-3.92
50	5.92	-2.02	7.24	-3.34	8.57	-4.67	9.19	-1.40	7.02	-3.56
60	5.22	-1.63	6.36	-2.76	7.50	-3.90	8.14	-1.00	6.07	-3.05
70	4.27	-1.24	5.18	-2.14	6.10	-3.05	6.69	- .65	4.90	-2.43
80	3.10	- .85	3.75	-1.50	4.41	-2.15	4.89	- .39	3.52	-1.74
90	1.72	- .47	2.08	- .82	2.45	-1.17	2.71	- .22	1.93	- .97
95	.94	- .28	1.14	- .48	1.34	- .68	1.47	- .16	1.05	- .56
100	(.10)	(-.10)	(.13)	(-.13)	(.16)	(-.16)	(.13)	(-.13)	(.13)	(-.13)
100	-	.00	-	.00	-	.00	-	.00	-	.00

TABLE I - CONTINUED

Ordinates of the Airfoils in Per Cent of the Chord - Continued

Airfoil	NACA 2512		NACA 6512		NACA 4509		NACA 4512		NACA 4518	
L.E. Radius	1.576		1.576		0.887		1.576		3.549	
Slope of radius passing through end of chord	2/25		6/25		4/25		4/25		4/25	
Stations	Upper	Lower	Upper	Lower	Upper	Lower	Upper	Lower	Upper	Lower
0	-	0.00	-	0.00	-	0.00	-	0.00	-	0.00
1-1/4	2.09	-1.70	2.57	-1.34	1.75	-1.12	2.33	-1.51	3.56	-2.25
2-1/2	2.91	-2.33	3.56	-1.82	2.47	-1.50	3.22	-2.07	4.79	-3.16
5	4.02	-3.09	5.02	-2.26	3.54	-1.84	4.50	-2.67	6.49	-4.27
7-1/2	4.83	-3.59	6.13	-2.43	4.36	-1.99	5.46	-2.99	7.74	-4.96
10	5.46	-3.92	7.06	-2.45	5.04	-2.05	6.25	-3.18	8.74	-5.41
15	6.40	-4.30	8.58	-2.27	6.12	-1.96	7.46	-3.28	10.25	-5.89
20	7.03	-4.43	9.69	-1.91	6.89	-1.75	8.34	-3.17	11.27	-6.01
25	7.44	-4.44	10.50	-1.47	7.46	-1.47	8.95	-2.95	11.96	-5.91
30	7.69	-4.33	11.07	- .98	7.85	-1.16	9.37	-2.66	12.37	-5.68
40	7.72	-3.90	11.56	- .06	8.19	- .52	9.64	-1.97	12.53	-4.89
50	7.29	-3.29	11.29	.71	7.97	.03	9.29	-1.29	11.94	-3.94
60	6.49	-2.63	10.35	1.21	7.27	.42	8.43	- .70	10.72	-2.98
70	5.35	-1.97	8.76	1.39	6.12	.62	7.06	- .29	8.92	-2.11
80	3.92	-1.33	6.54	1.24	4.56	.60	5.23	- .04	6.57	-1.34
90	2.18	- .72	3.68	.72	2.56	.35	2.93	.00	3.69	- .71
95	1.19	- .42	2.00	.33	1.38	.15	1.58	- .04	2.01	- .44
100	(.13)	(-.13)	(.12)	(-.12)	(.09)	(-.09)	(.12)	(-.12)	(.19)	(-.19)
100	-	.00	-	.00	-	.00	-	.00	-	.00

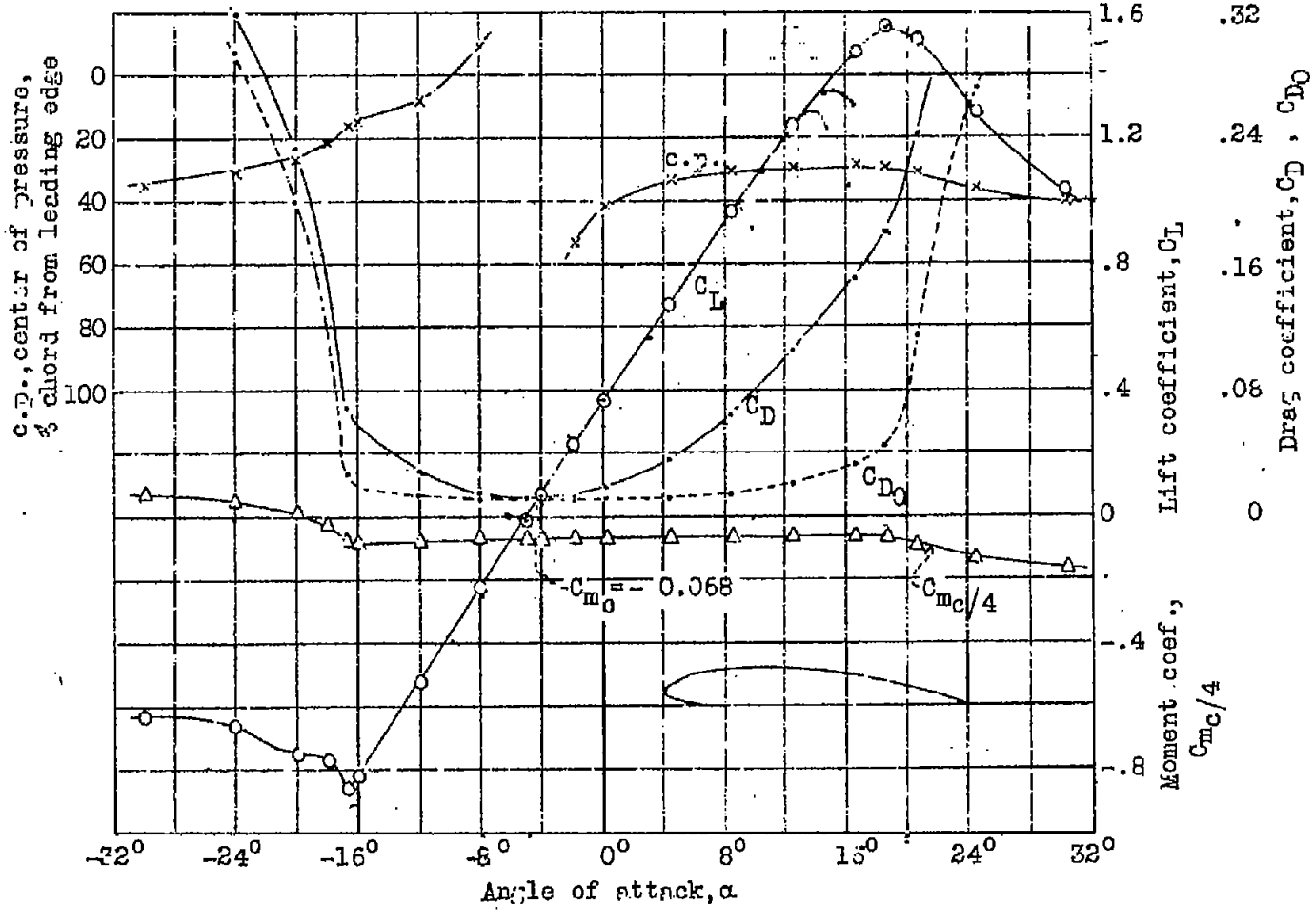

Fig.1 Airfoil, Clark Y. Reynold's Number 3,100,000. V.D.T. tests, 525 and 698. Aspect ratio 6. Tunnel wall correction applied. Dates, 3/31 , 10/31 .

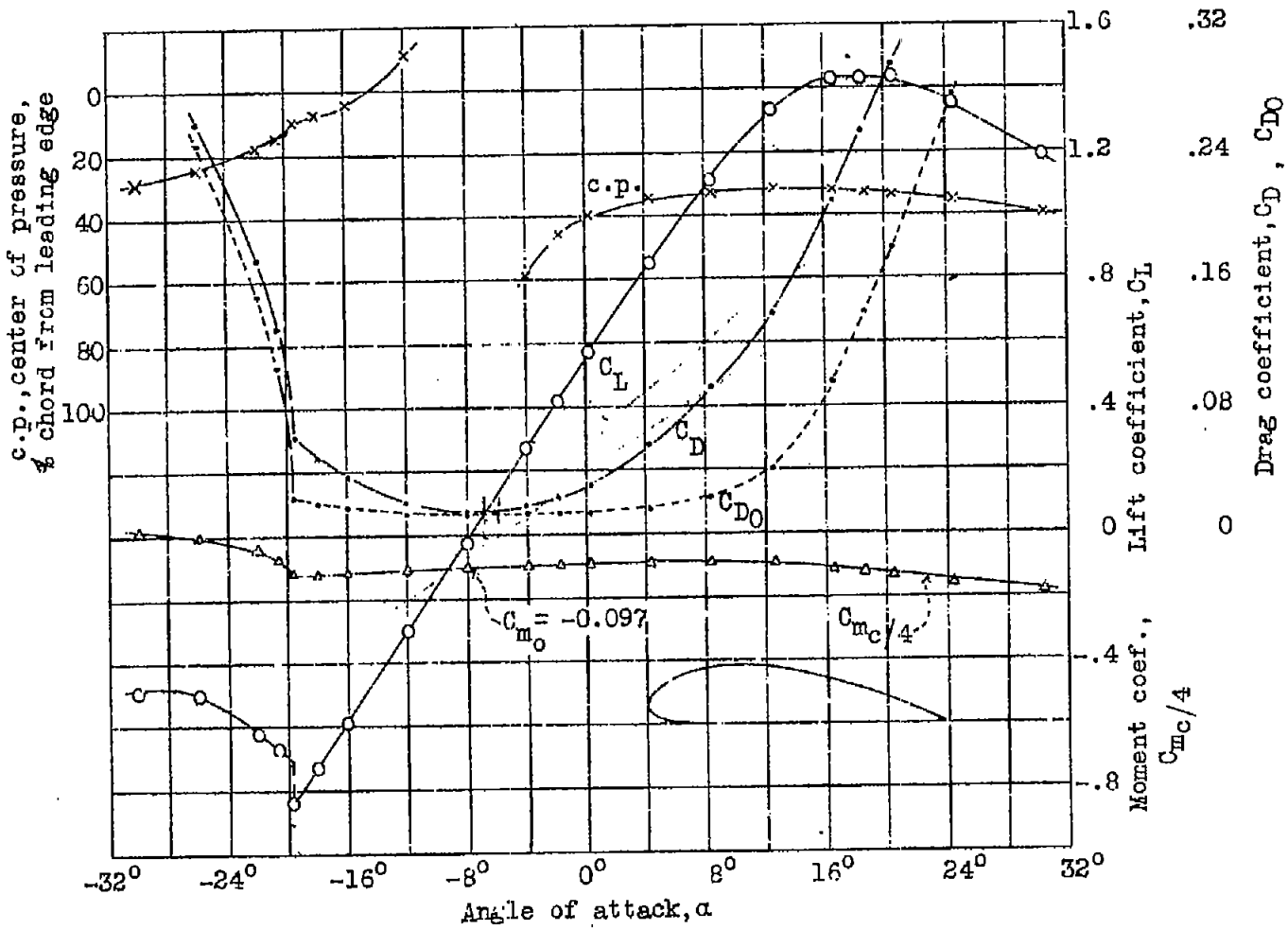

Fig.2 Airfoil, Clark Y-18. Reynold's Number 3,100,000. V.D.T. tests, 693 and 642. Aspect ratio 6. Tunnel wall correction applied. Dates, 10/31 and 7/31.

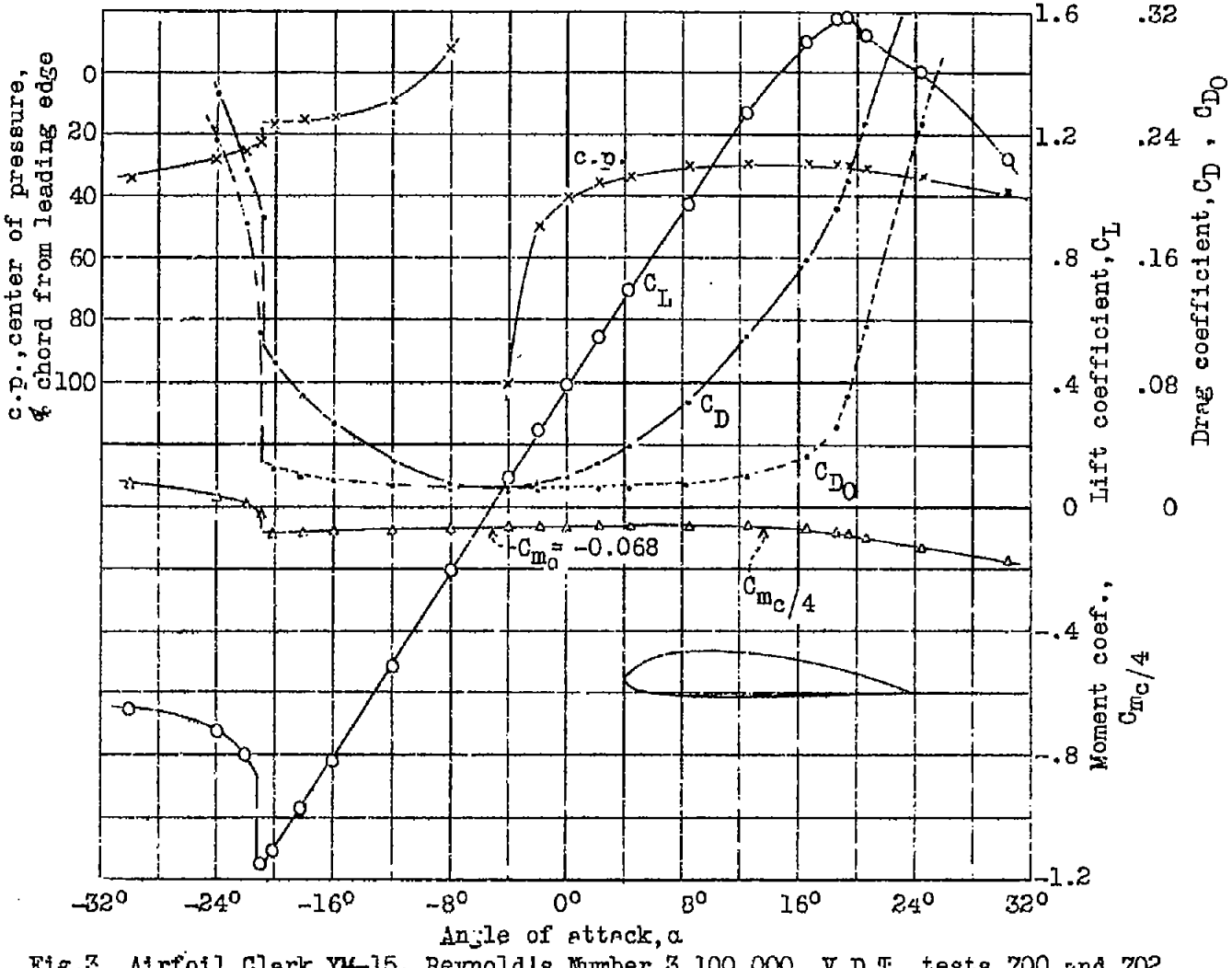

Fig.3 Airfoil, Clark YM-15. Reynold's Number 3,100,000. V.D.T. tests, 700 and 702. Aspect ratio 6. Tunnel wall correction applied. Date, 10/31.

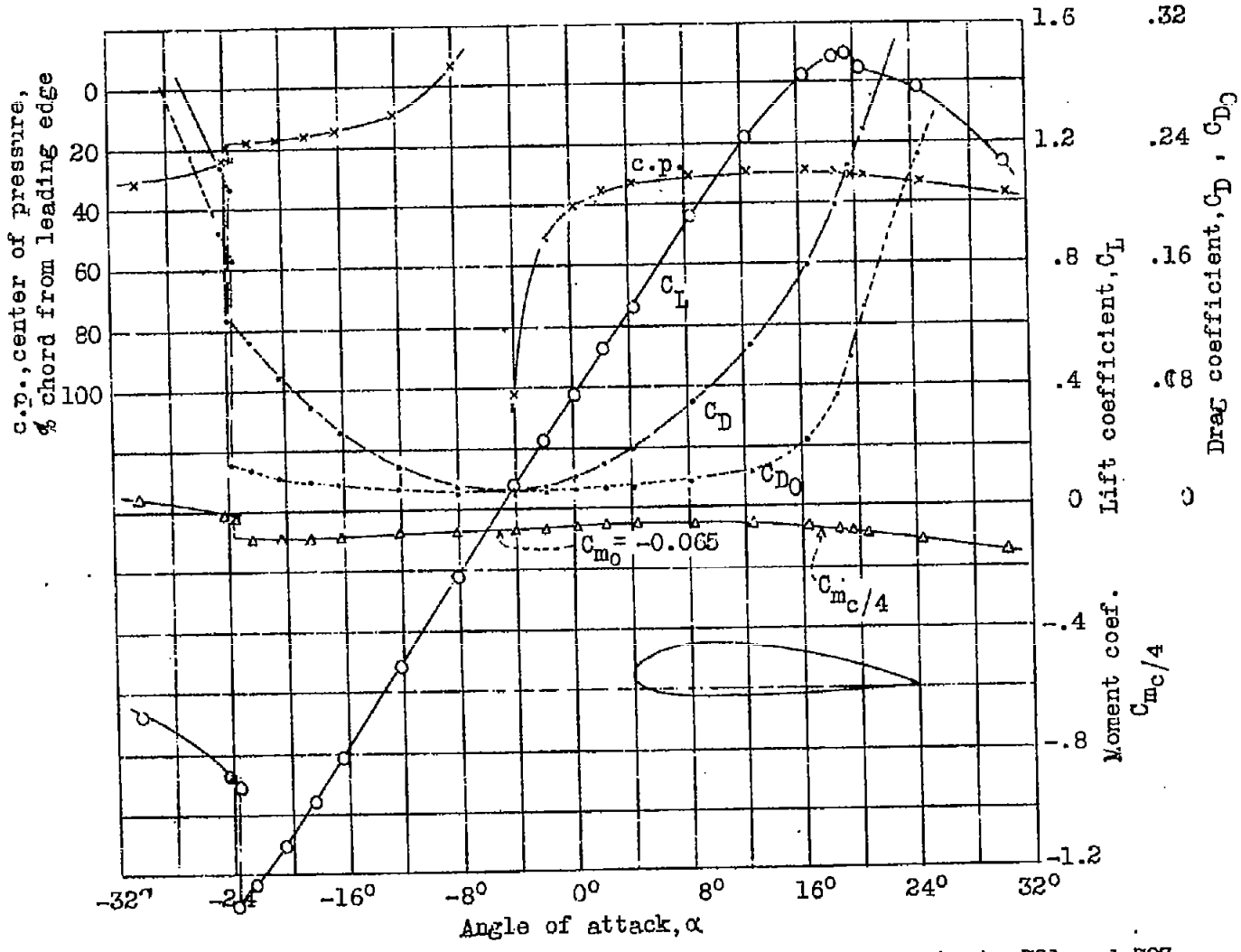

Fig.4 Airfoil, Clark YM-18. Reynolds Number 3,100,000. V.D.T. tests, 701 and 703. Aspect ratio 6. Tunnel wall correction applied. Date, 10/31

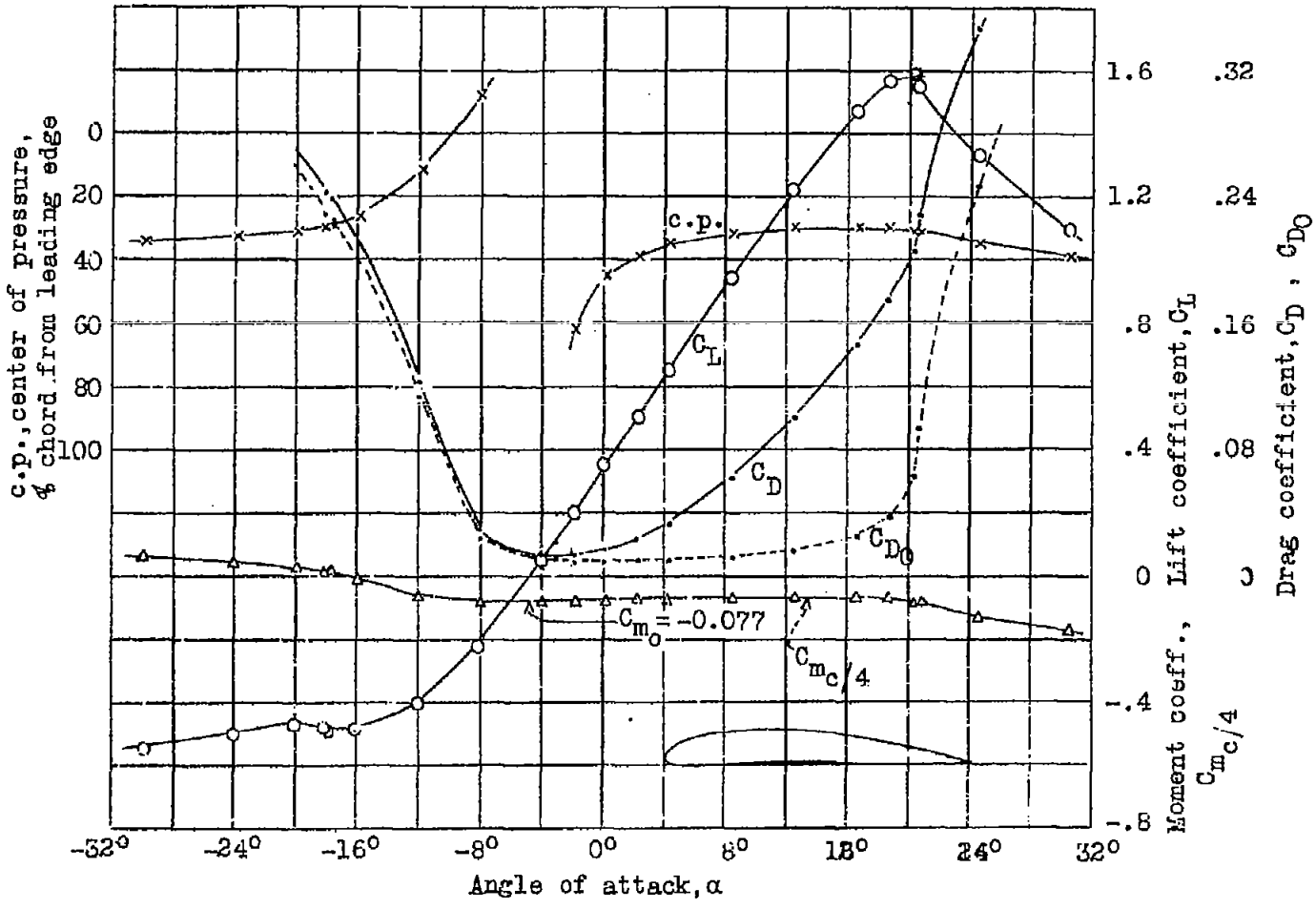

Fig.5 Airfoil U.S.A. 27. Reynolds Number 3,100,000. V.D.T. tests, 694 and 696. Aspect ratio 6. Tunnel wall correction applied. Date, 10/31.

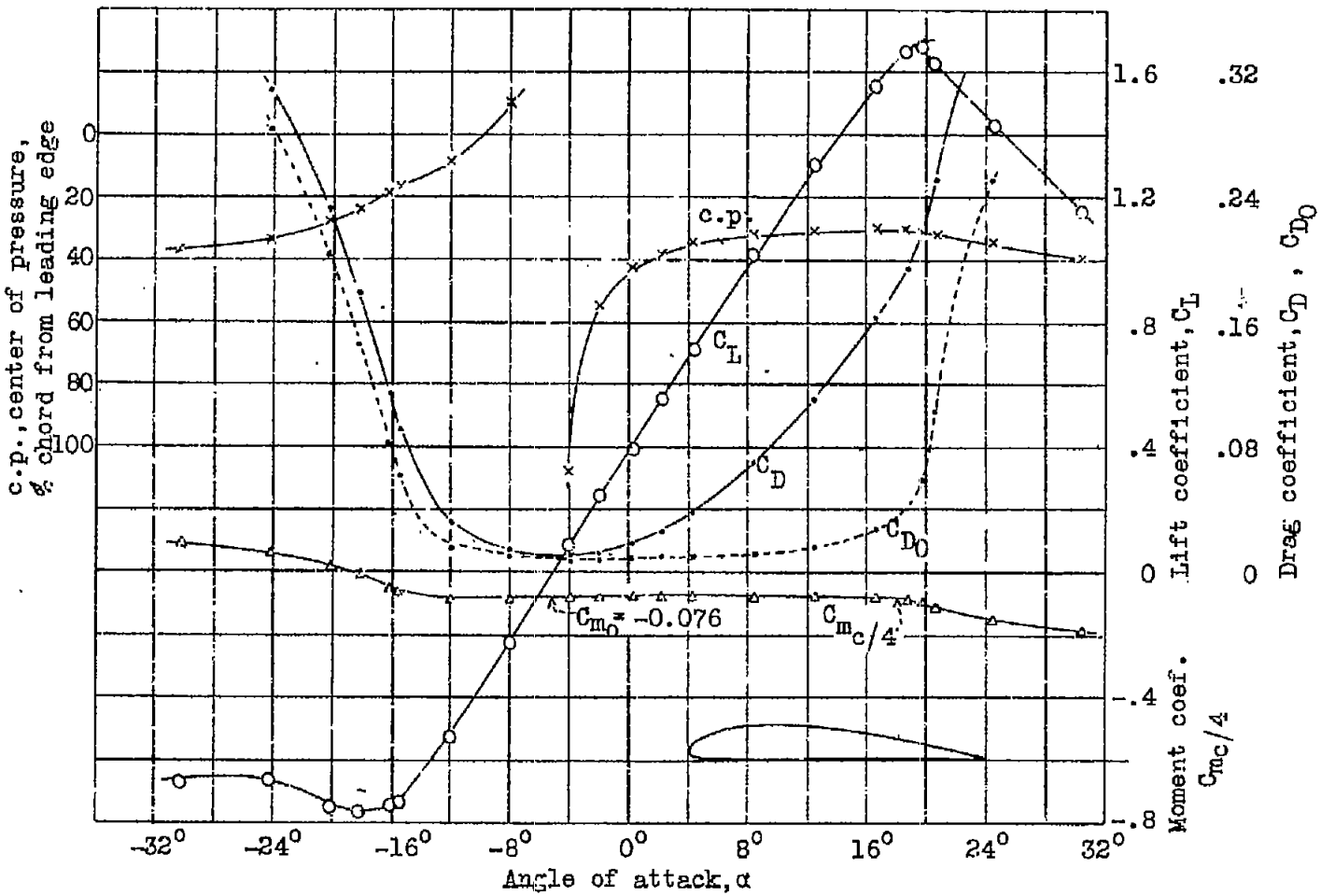

Fig.6 Airfoil, U.S.A. 35B. Reynold's Number 3,100,000. V.D.T. tests, 695 and 697. Aspect ratio 6. Tunnel wall correction applied. Date, 10/31.

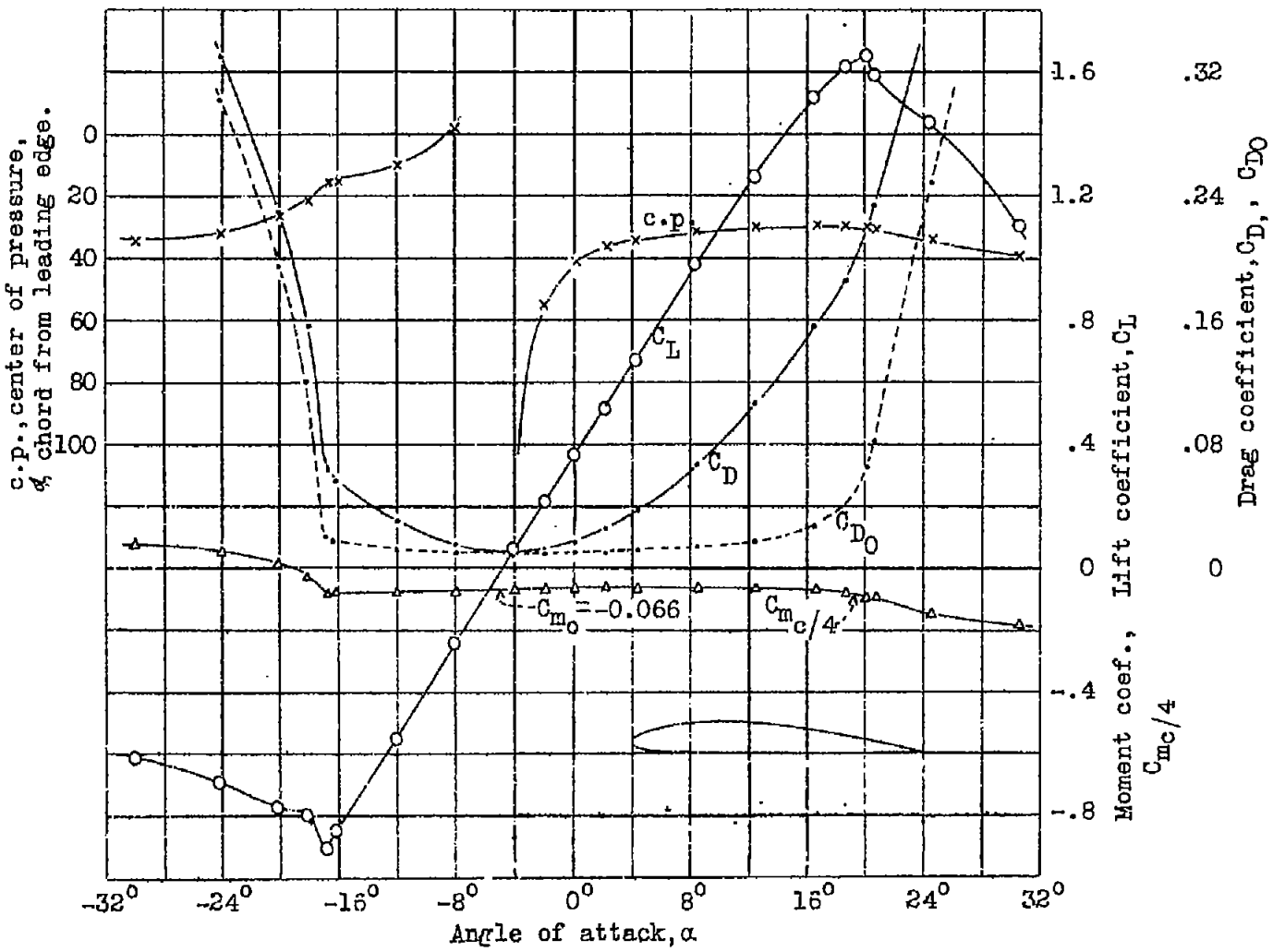

Fig. 7 Airfoil, Boeing 103. Reynold's Number 3,100,000. V.D.T. tests 704 and 706 Aspect ratio 6. Tunnel wall correction applied. Date 10/31.

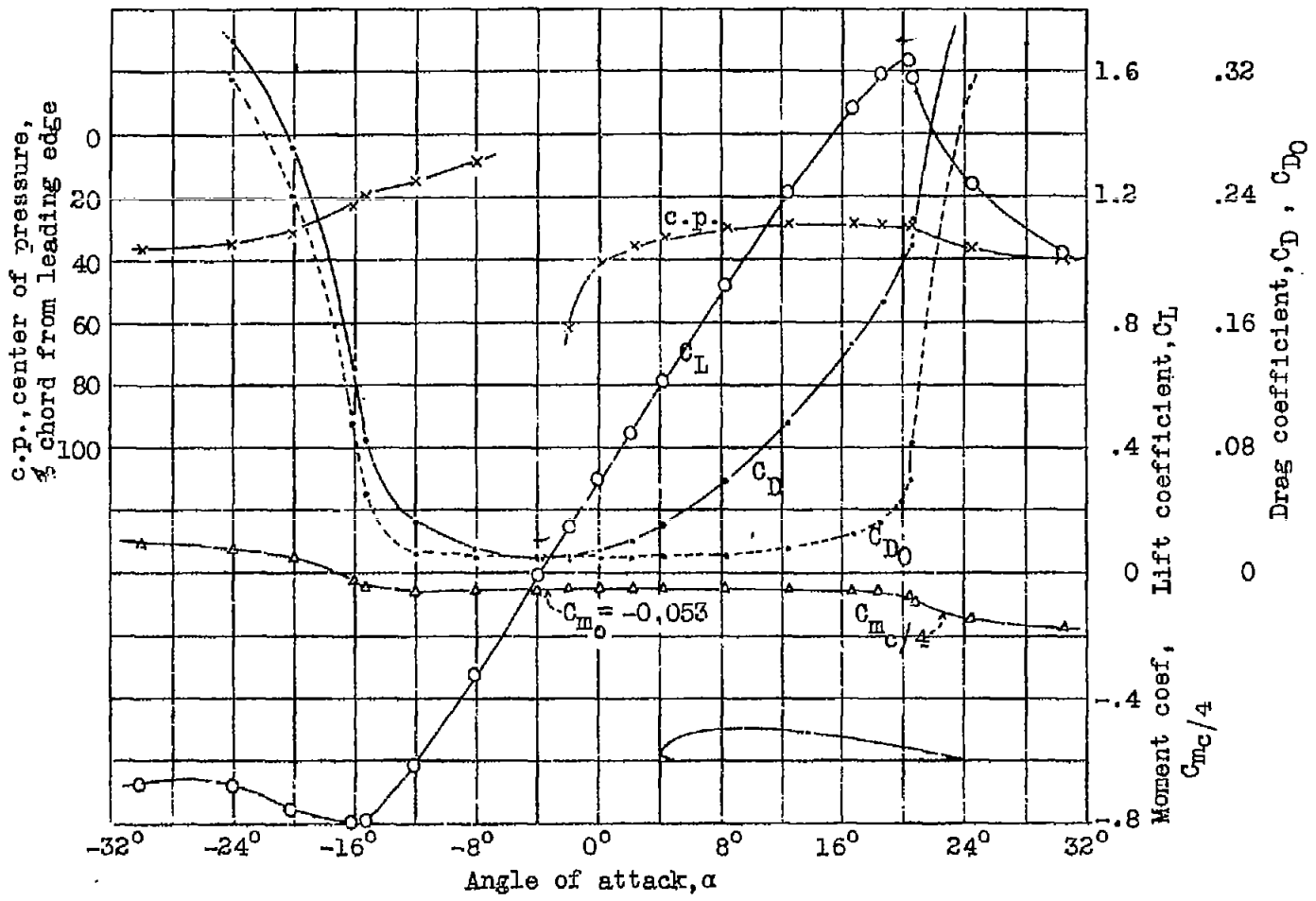

Fig.8 Airfoil, Boeing 103A Reynold's Number 3,100,000. V.D.T. tests, 707 and 709. Aspect ratio 6. Tunnel wall correction applied. Date, 10/31.

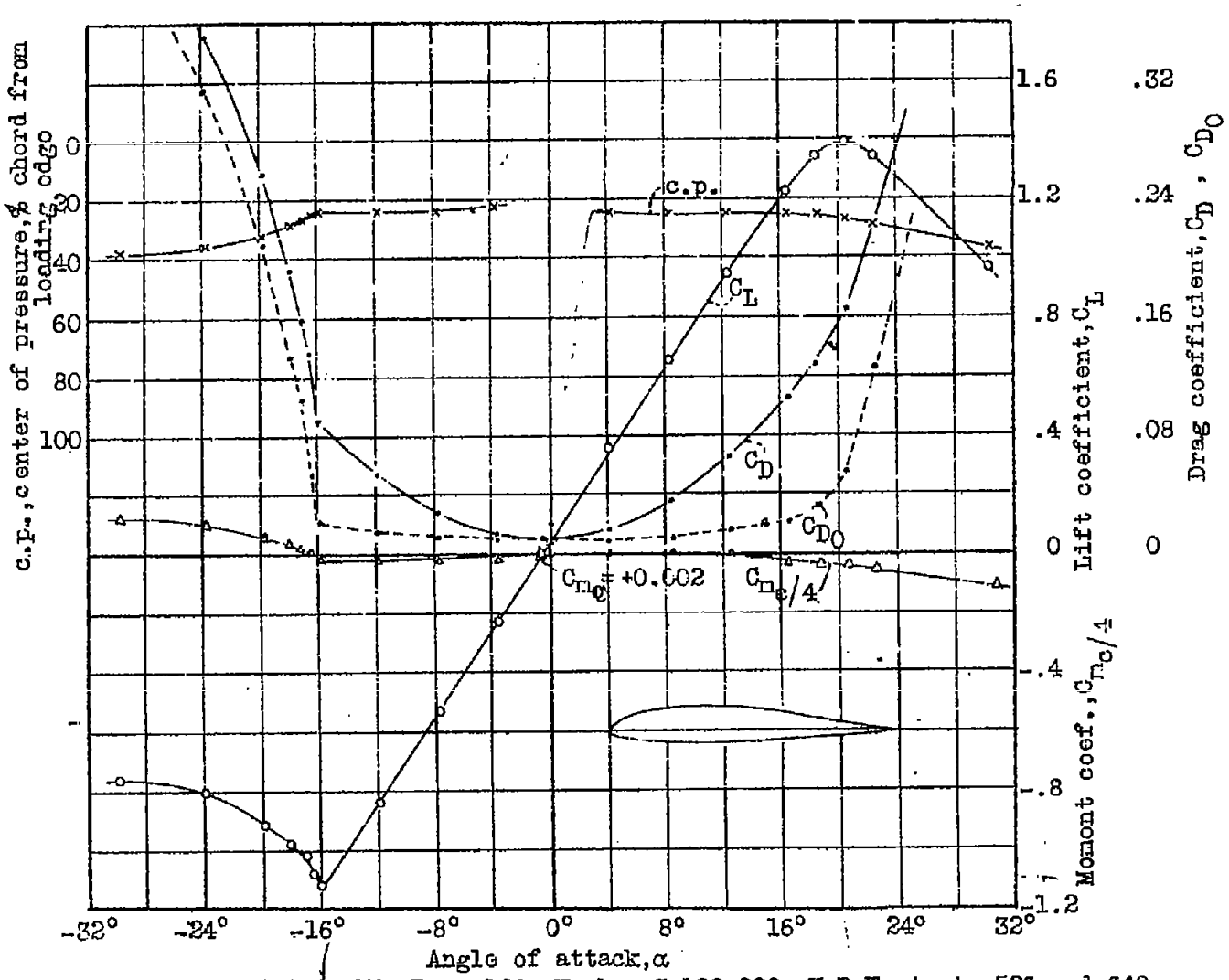

Fig.9 Airfoil, N.A.C.A. M6. Reynold's Number 3,100,000. V.D.T. tests, 526 and 640. Aspect ratio, 6. Tunnel wall correction applied. Dates, 3/31 and 7/31.

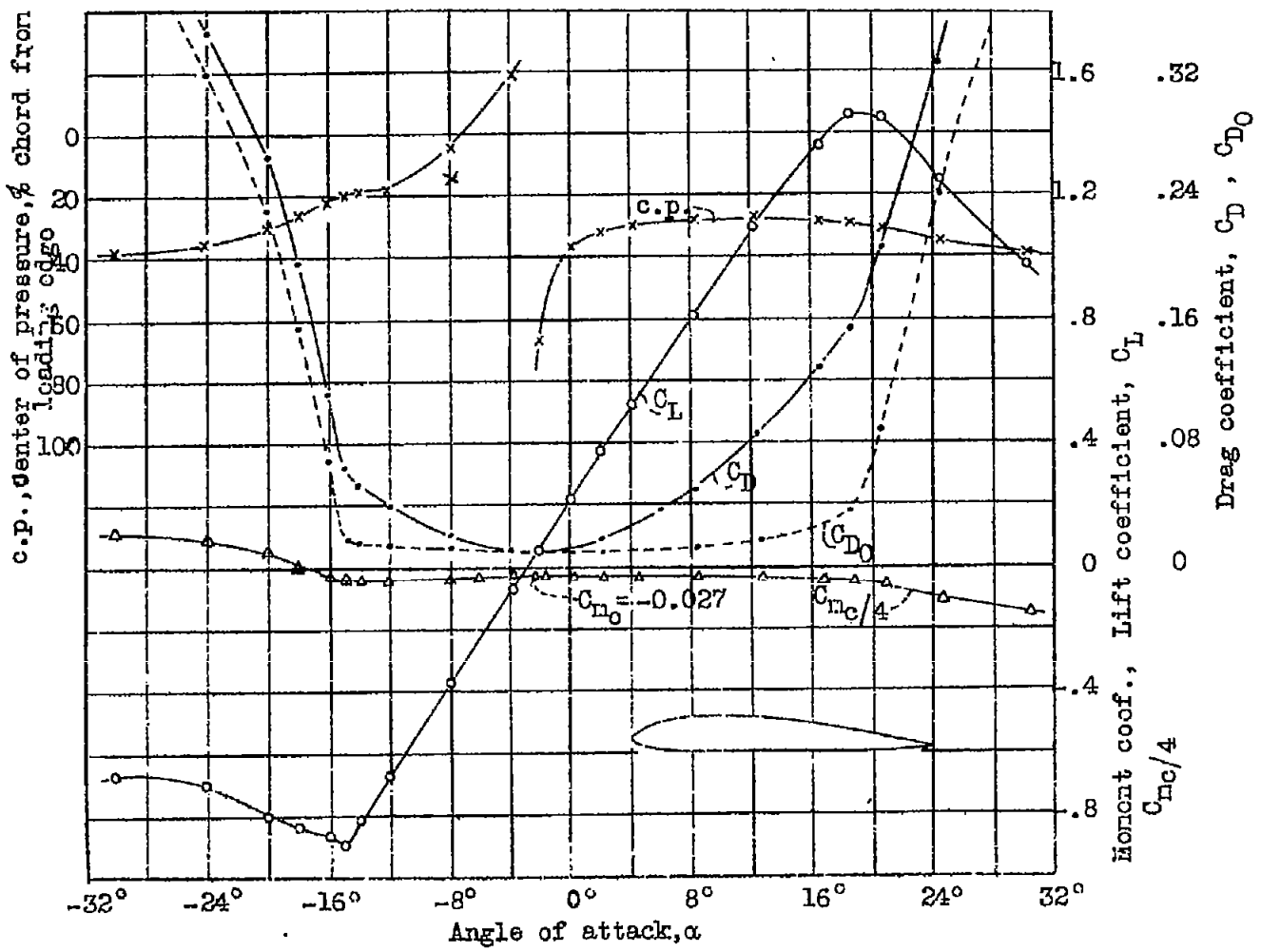

Fig.10 Airfoil, N.A.C.A. CYH. Reynold's Number 3,100,000. V.D.T. tests, 536 and 641. Aspect ratio, 6. Tunnel wall correction applied. Dates, 3/31 and 7/31.

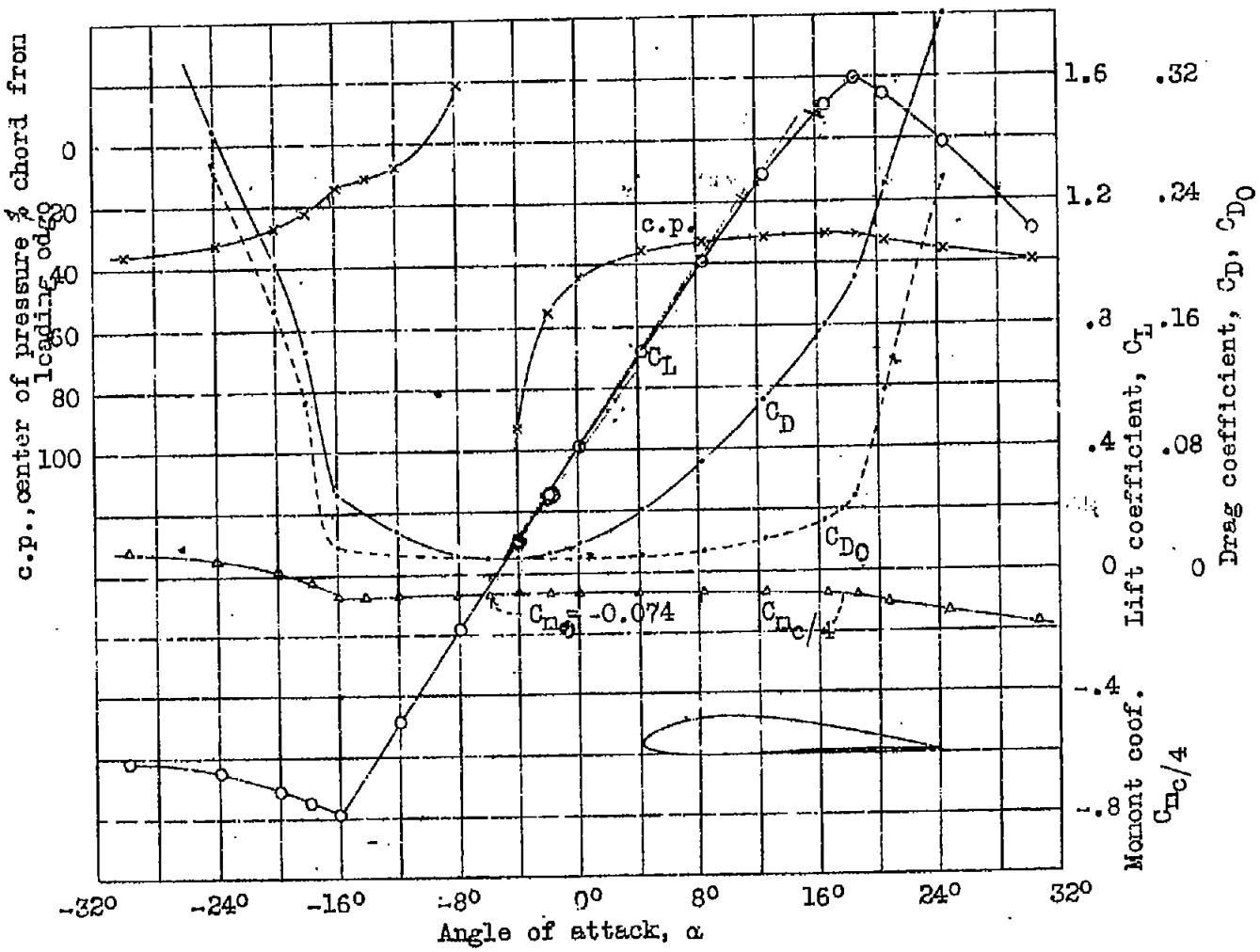

Fig.11 Airfoil, N 22. Reynold's Number, 3,100,000. V.D.T. tests, 542 and 638. Aspect ratio, 6. Dates 3/31 and 7/31. Tunnel wall correction applied.

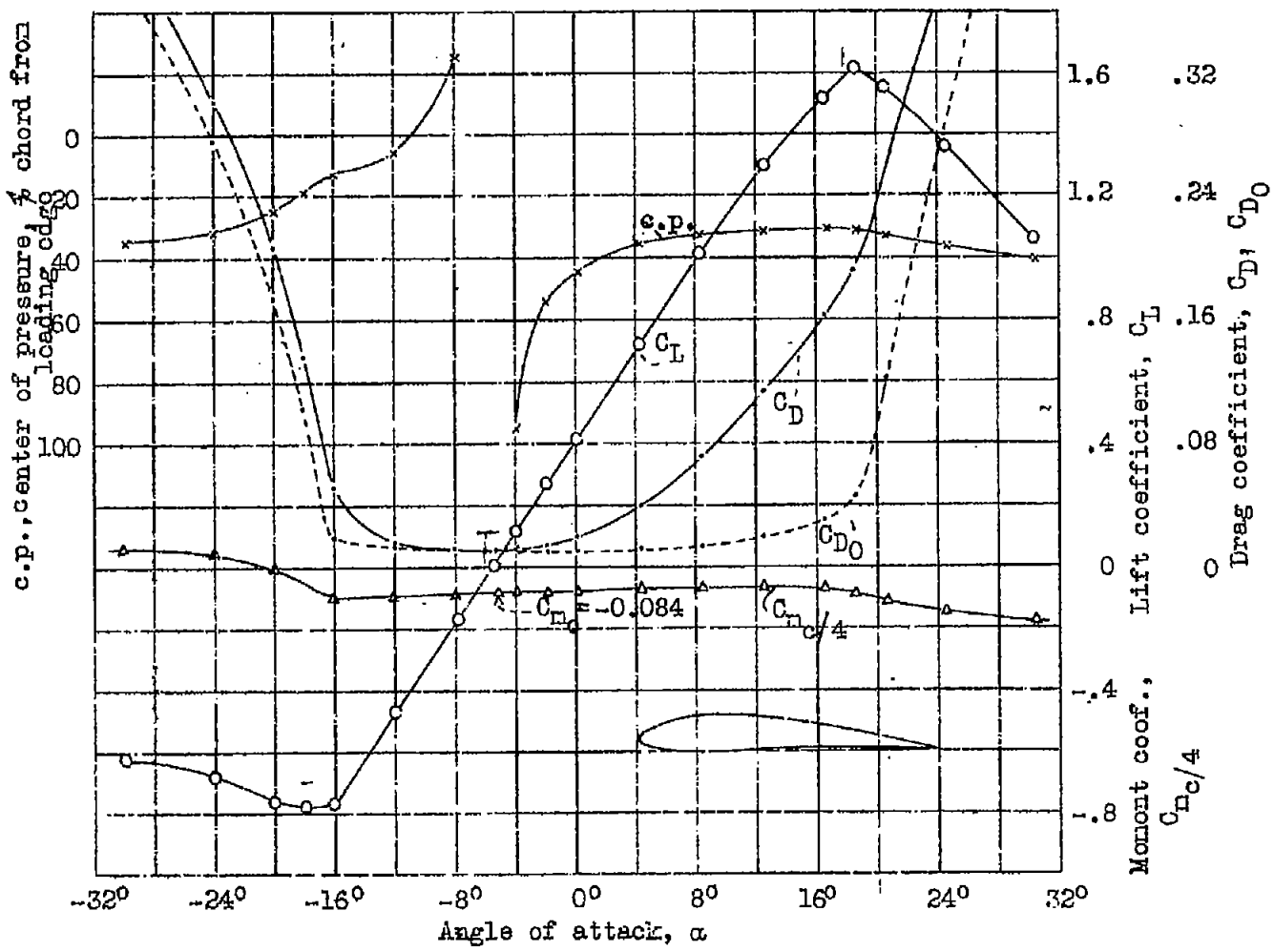

Fig.12 Airfoil, C 72. Reynold's Number, 3,100,000. V.D.T. tests, 529 and 637. Aspect ratio, 6. Dates 3/31 and 7/31. Tunnel wall correction applied.

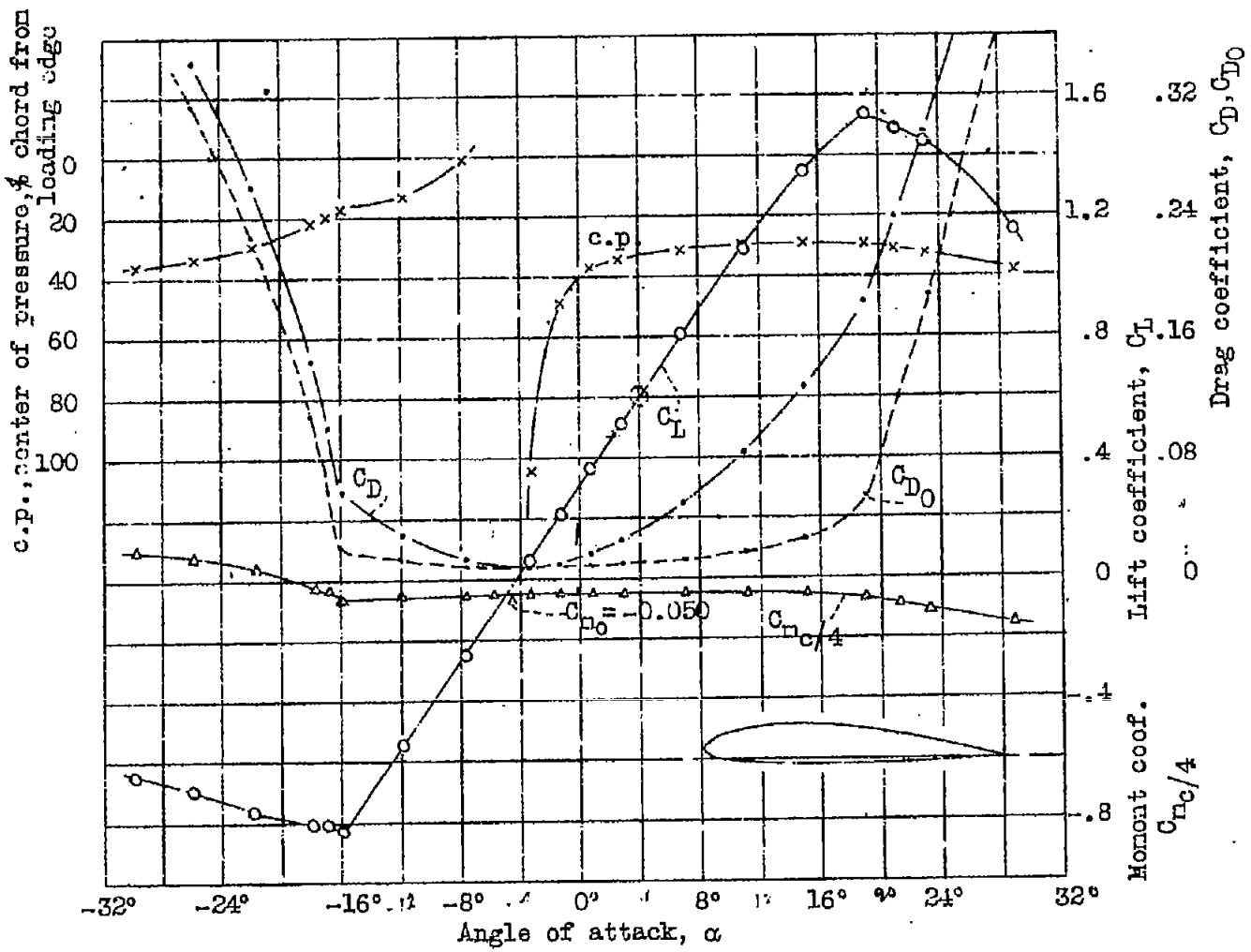

Fig. 13 Airfoil, Boeing 106. Reynold's Number, 3,100,000. V.D.T. tests, 531 and 635, Aspect ratio, 6. Dates 3/31 and 7/31. Tunnel wall correction applied.

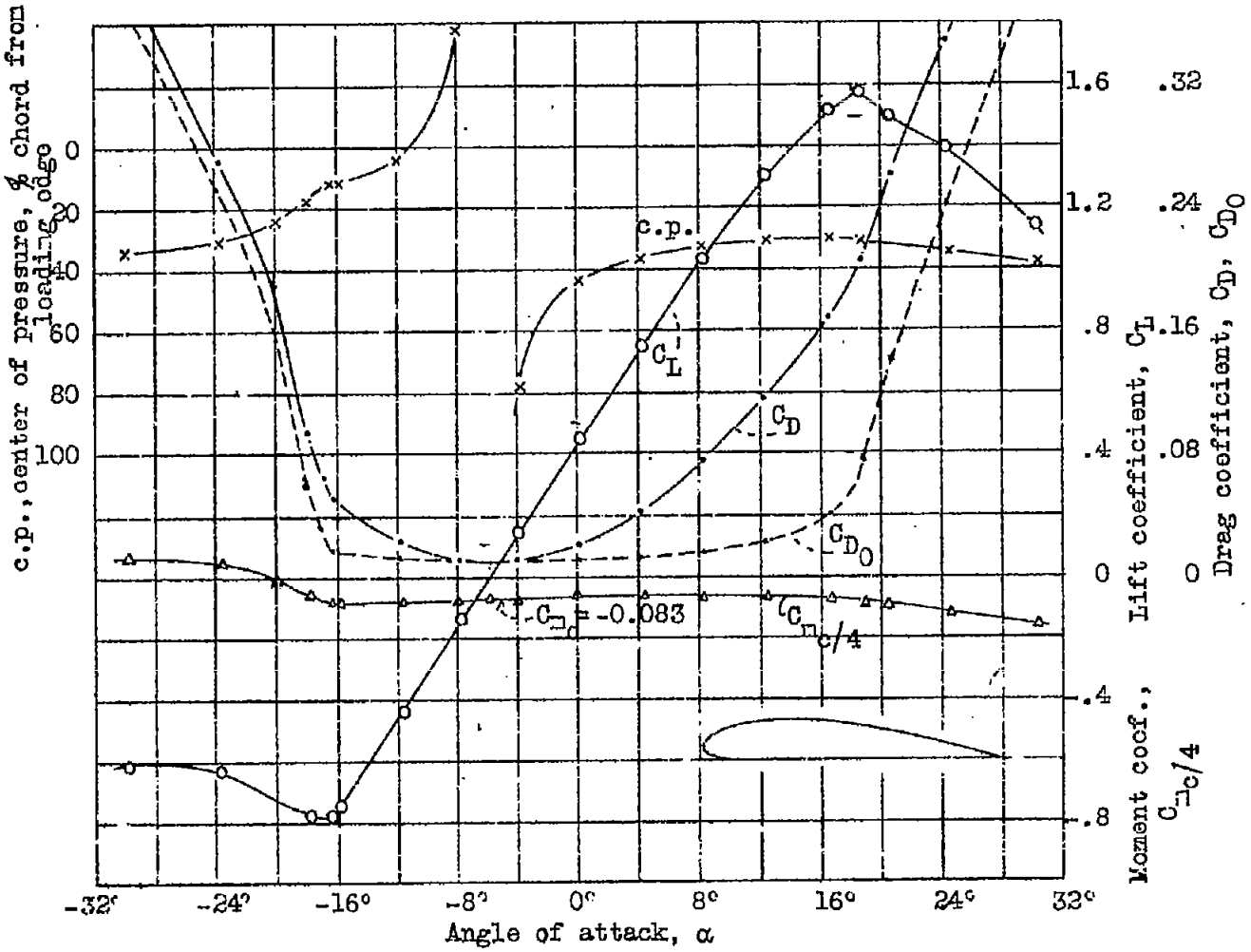

Fig. 14 Airfoil, Gött. 398. Reynold's Number, 3,100,000. V.D.T. tests, 524 and 639. Aspect ratio, 6. Dates 3/31 and 7/31. Tunnel wall correction applied.

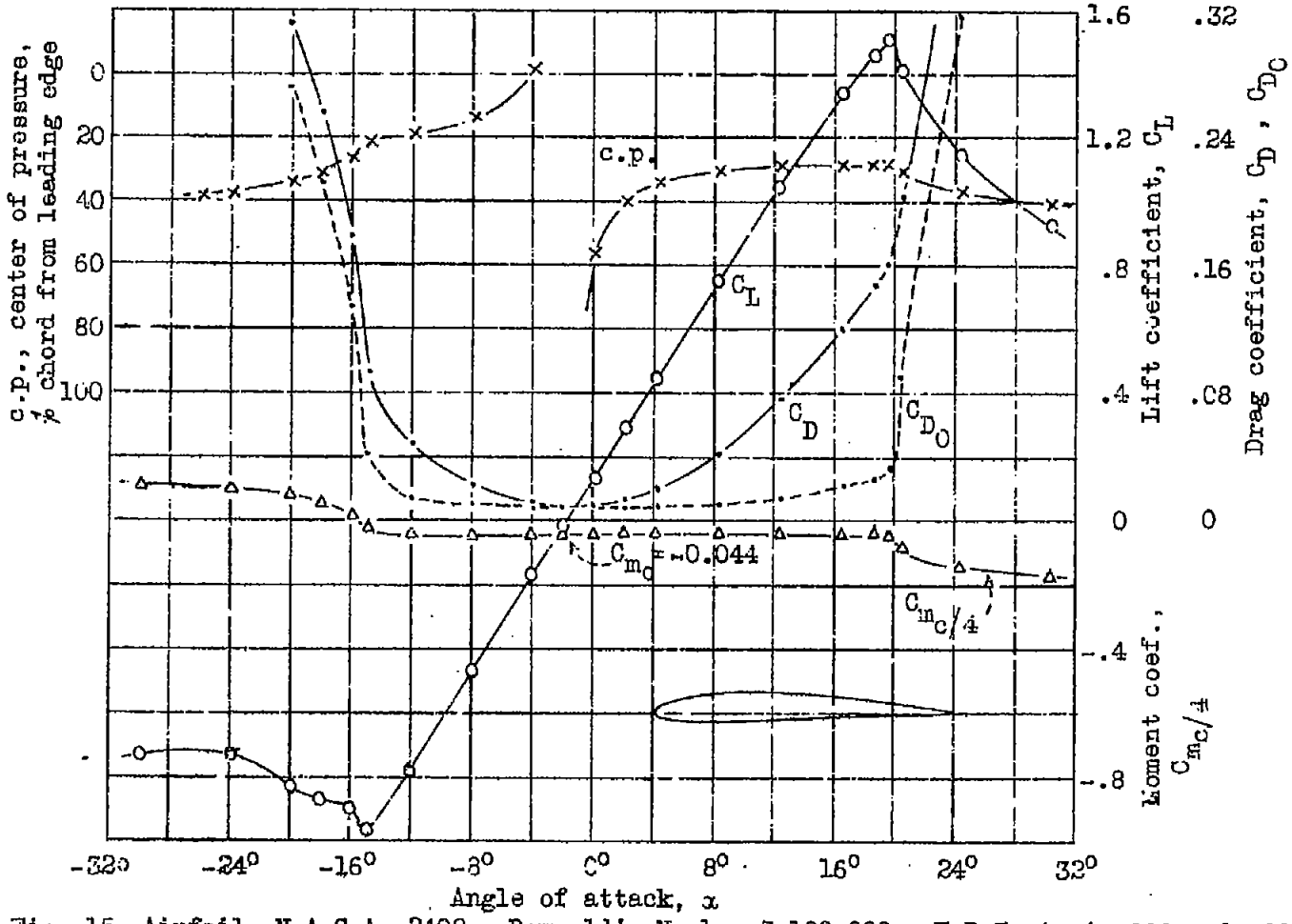

Fig. 15 Airfoil, N.A.C.A. 2409. Reynold's Number 3,100,000. V.D.T. tests, 666 and 699. Aspect ratio, 6. Tunnel wall correction applied. Dates, 9/31 and 10/31.

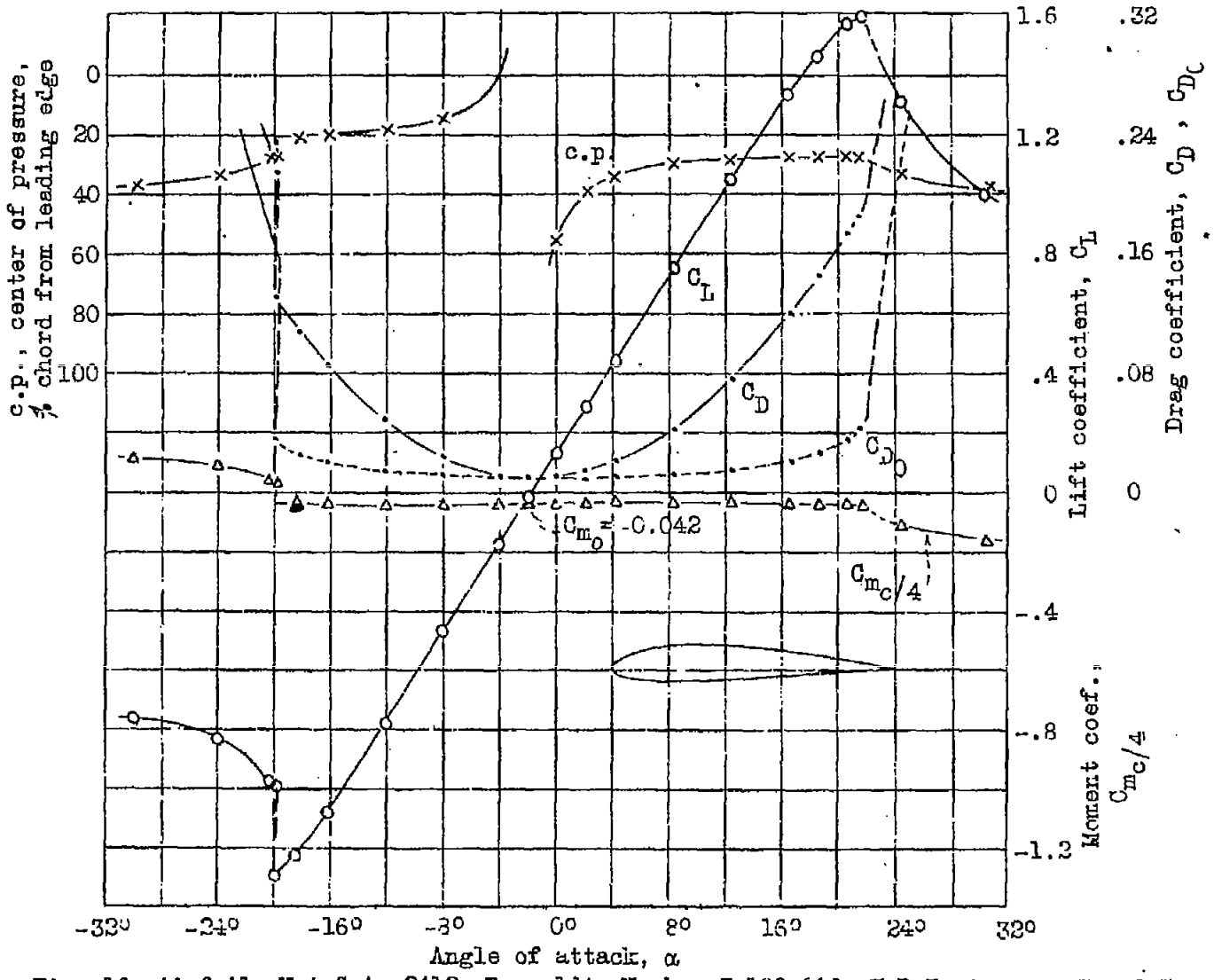

Fig. 16 Airfoil, N.A.C.A. 2412. Reynold's Number 3,100,000. V.D.T. tests,667 and 705. Aspect ratio, 6. Tunnel wall correction applied. Dates, 9/31 and 10/31.

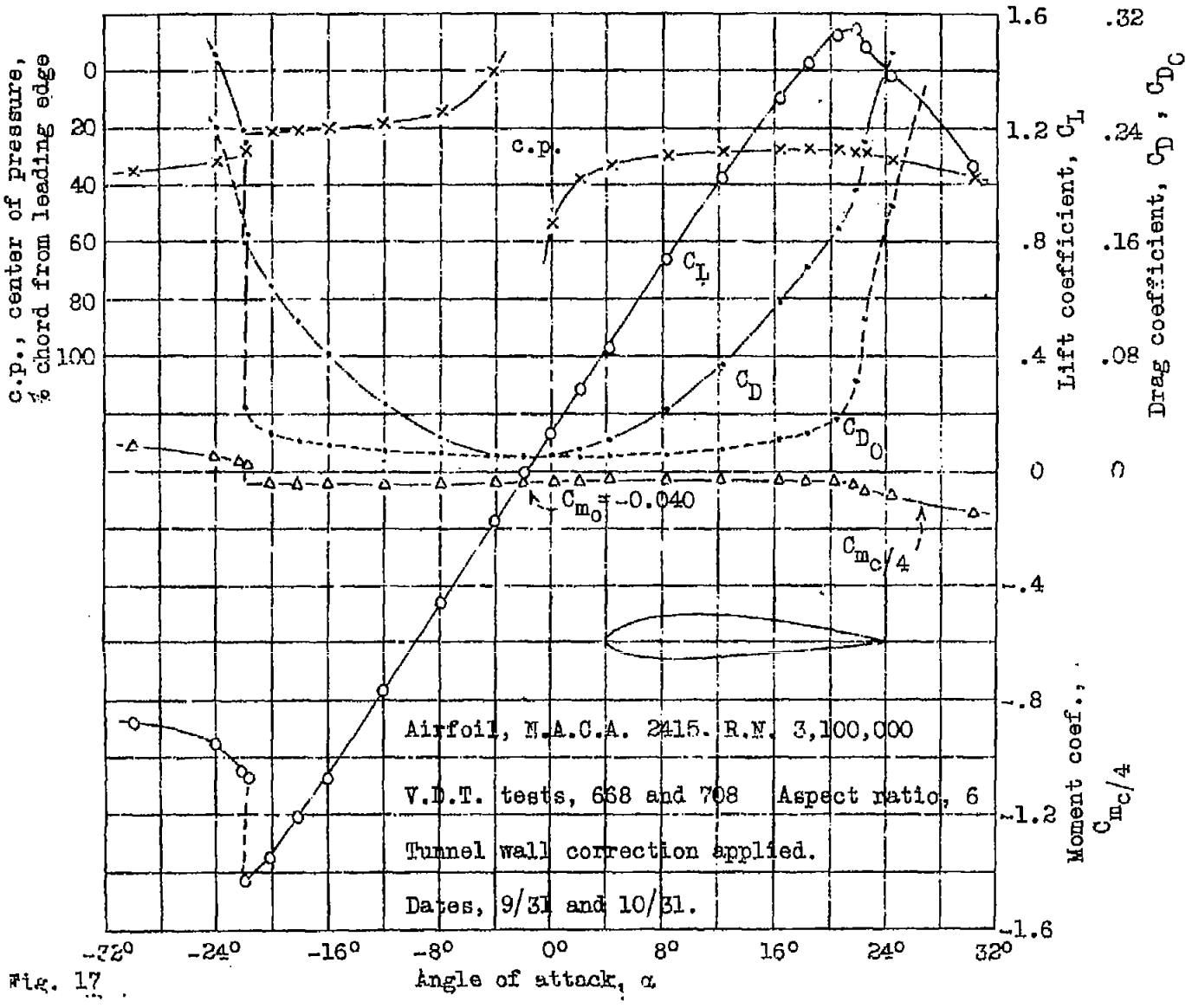
c.p., center of pressure, % chord from leading edge
0
20
40
60
80
100
c.p.
C_L
C_D
C_{D_0}
$C_{m_0} = -0.040$
$C_{m_{c/4}}$
Airfoil, N.A.C.A. 2415. R.N. 3,100,000
V.D.T. tests, 668 and 708 Aspect ratio, 6
Tunnel wall correction applied.
Dates, 9/31 and 10/31.
-32°
-24°
-16°
-8°
0°
8°
16°
24°
32°
Angle of attack, α
1.6
1.2
.8
.4
0
-.4
-.8
-1.2
-1.6
Lift coefficient, C_L
.32
.24
.16
.08
0
Drag coefficient, C_D, C_{D_0}
Moment coef., $C_{m_{c/4}}$

Fig. 17

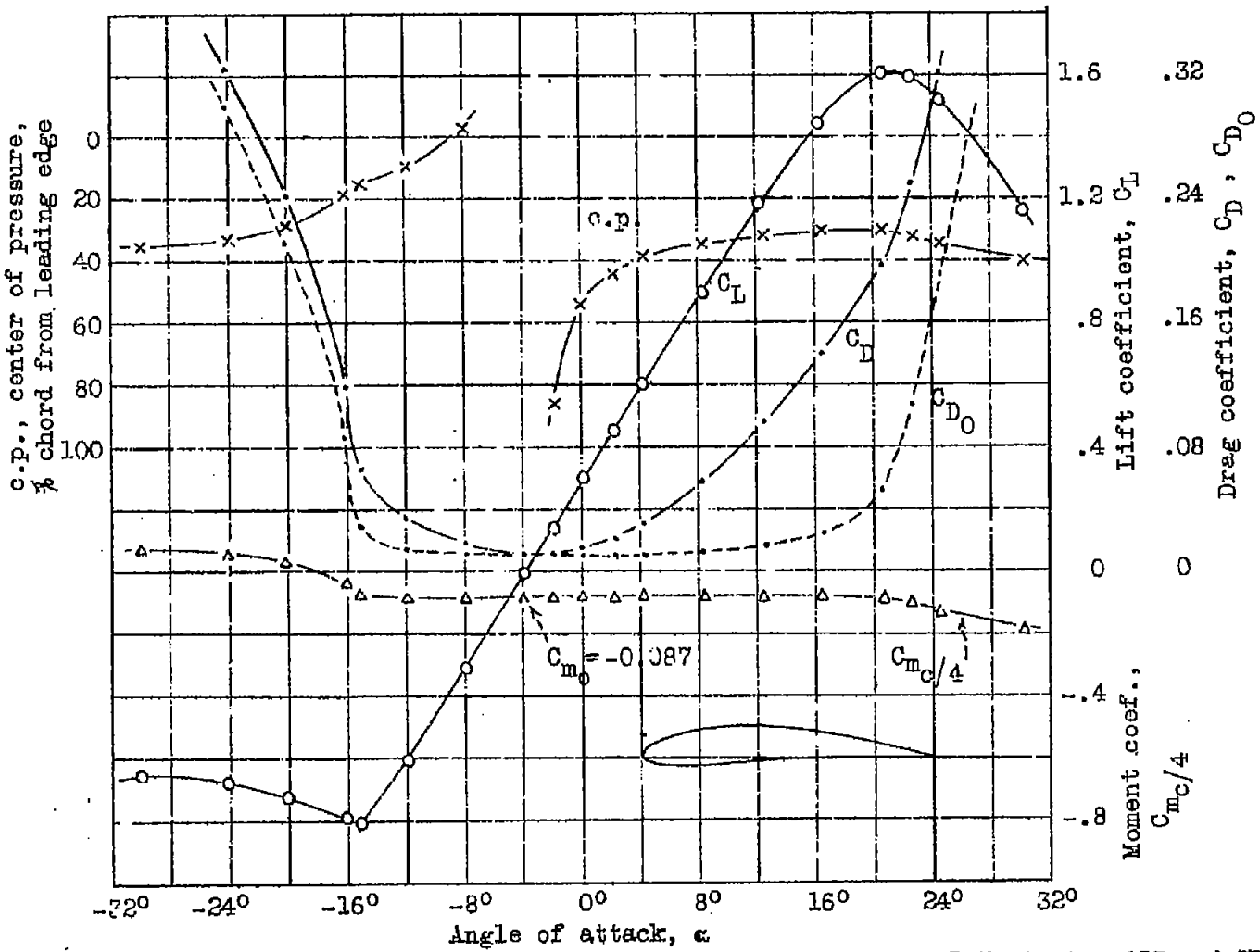

Fig. 18 Airfoil, N.A.C.A. 4412. Reynold's Number 3,100,000. V.D.T. tests, 653 and 712. Aspect ratio, 6. Tunnel wall correction applied. Dates, 8/31 and 10/31.

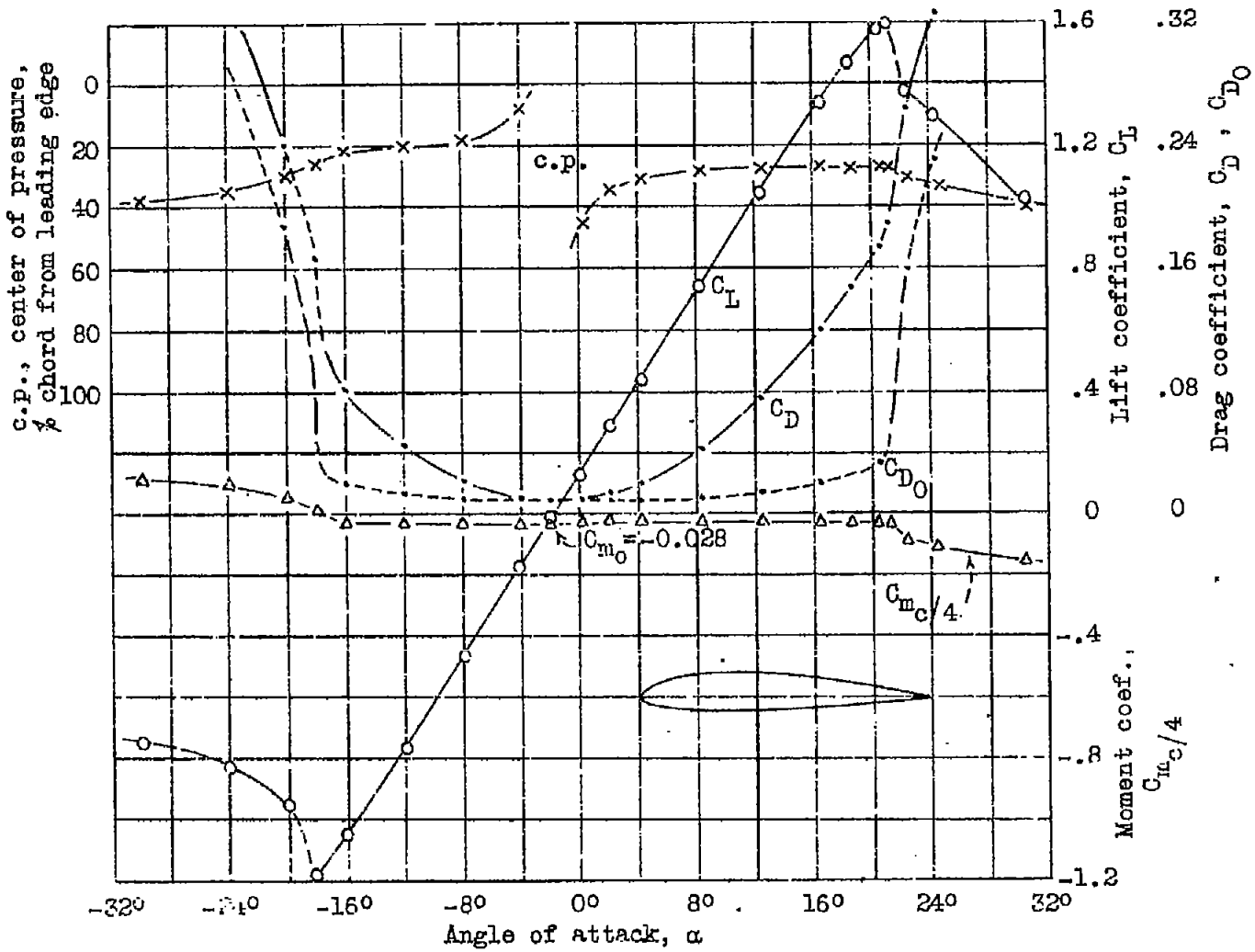

Fig. 19 Airfoil, N.A.C.A. 2212. Reynold's Number 3,100,000. V.D.T. tests, 685 and 711. Aspect ratio, 6. Tunnel wall correction applied. Dates, 9/31 and 10/31.

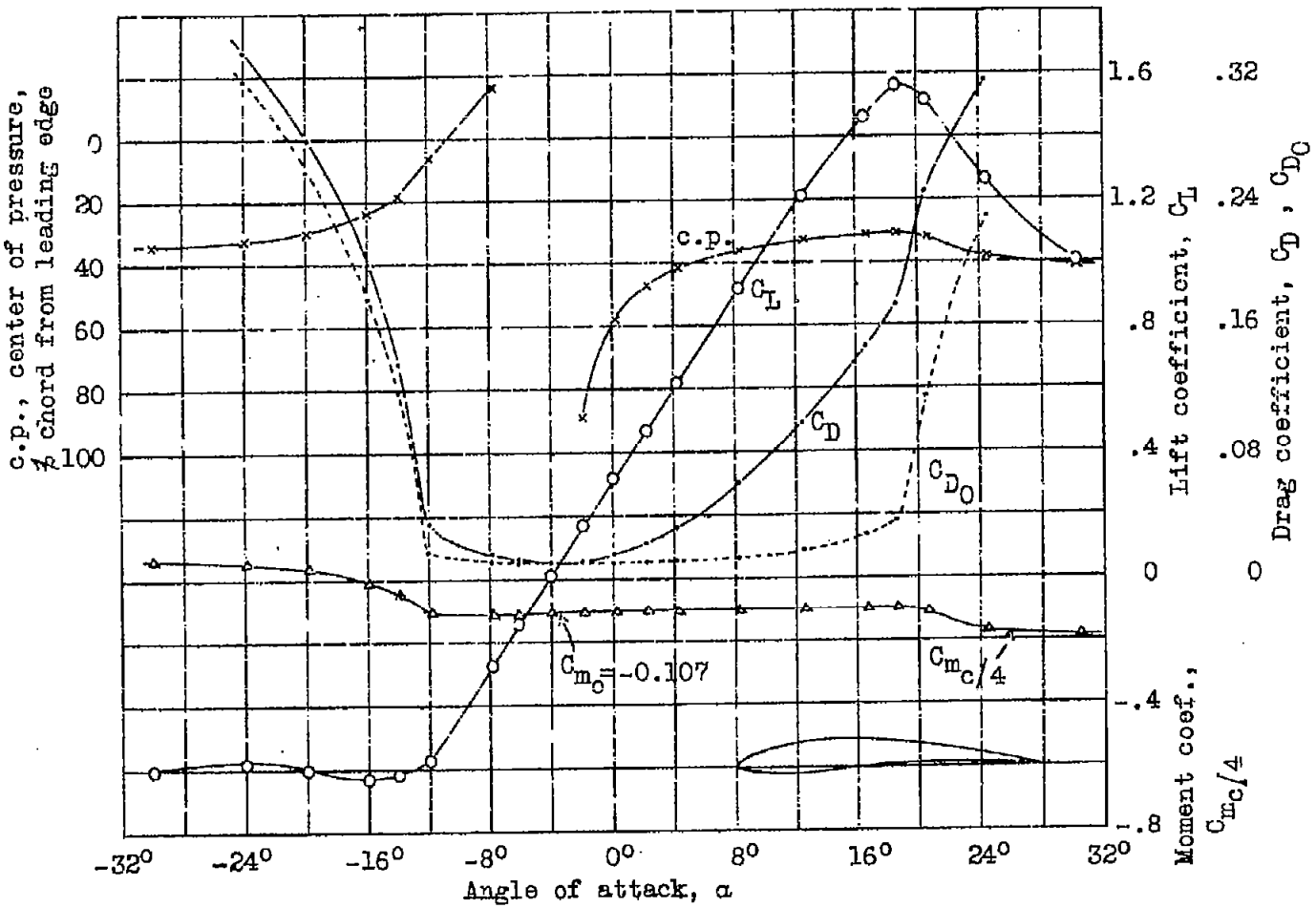

Fig. 20 Airfoil, N.A.C.A. 4509. Reynold's Number 3,100,000. V.D.T. tests, 569 and 644 Aspect ratio, 6. Tunnel wall correction applied. Dates, 4/31 and 7/31.

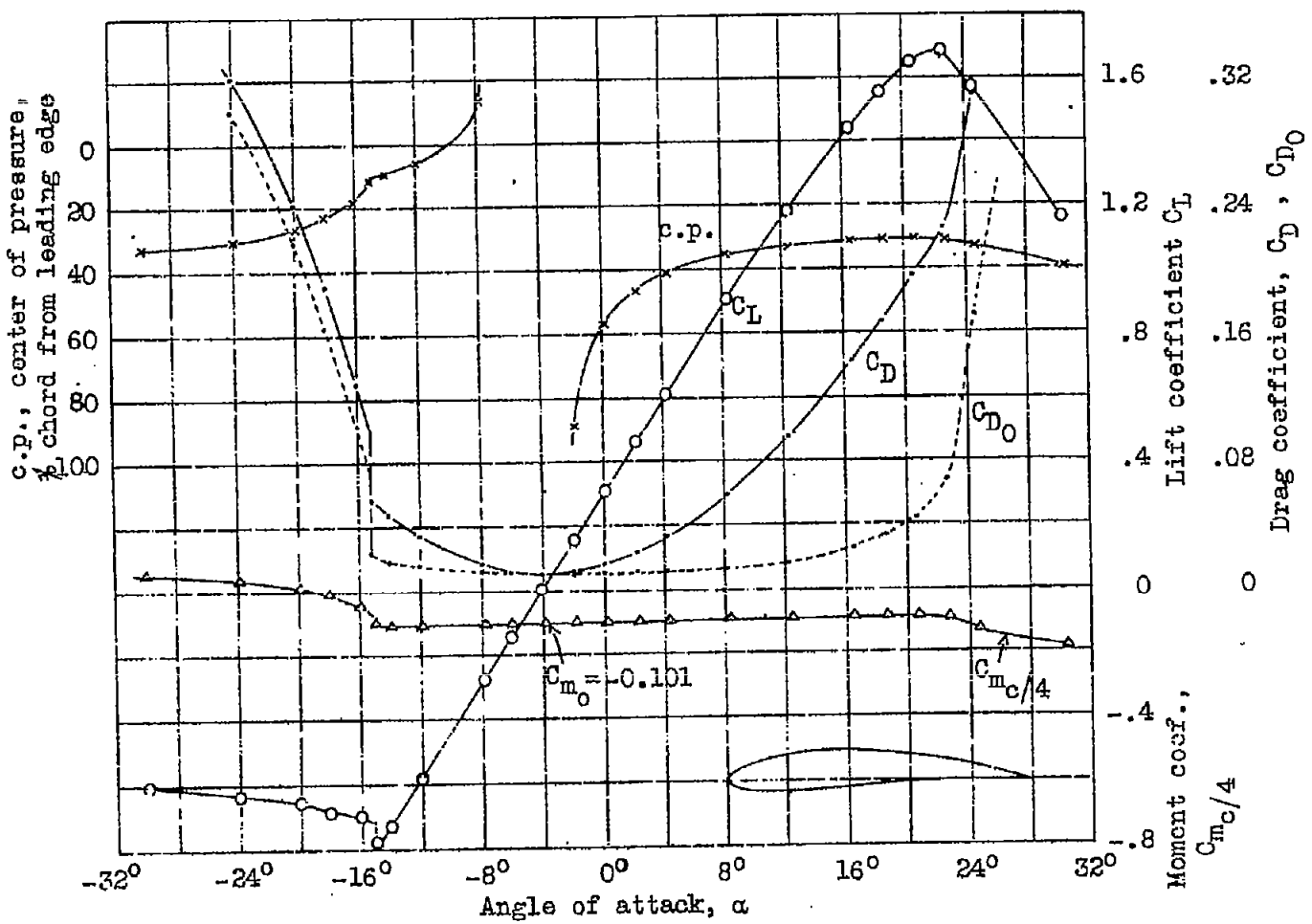

Fig.21 Airfoil, N.A.C.A. 4512. Reynold's Number 3,100,000. V.D.T. tests, 570 and 645. Aspect ratio, 6. Tunnel wall correction applied. Dates, 4/31 and 8/31.

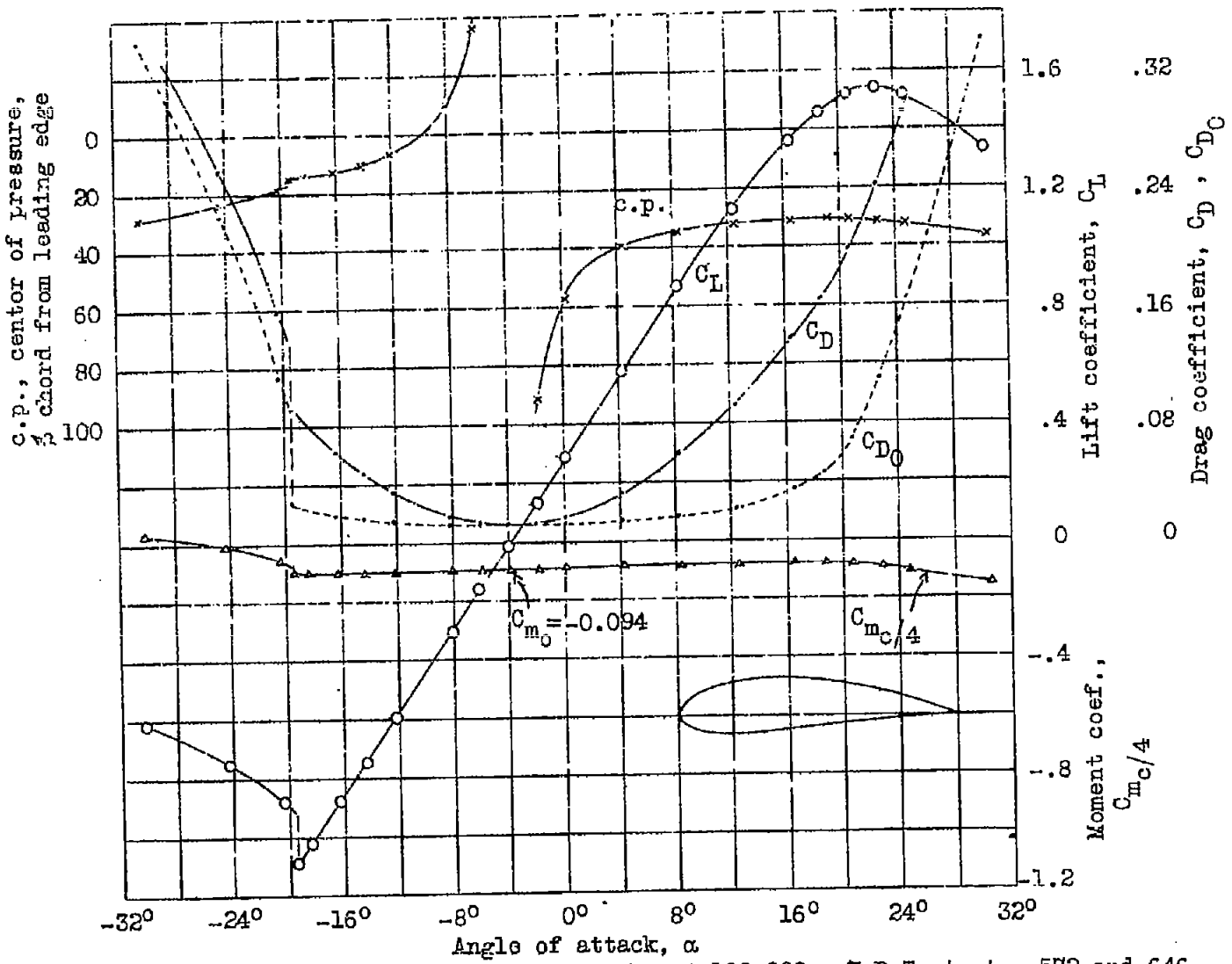

Fig. 22 Airfoil, N.A.C.A. 4518. Reynold's Number 3,100,000. V.D.T. tests, 572 and 646. Aspect ratio, 6. Tunnel wall correction applied. Dates, 4/31 and 8/31.

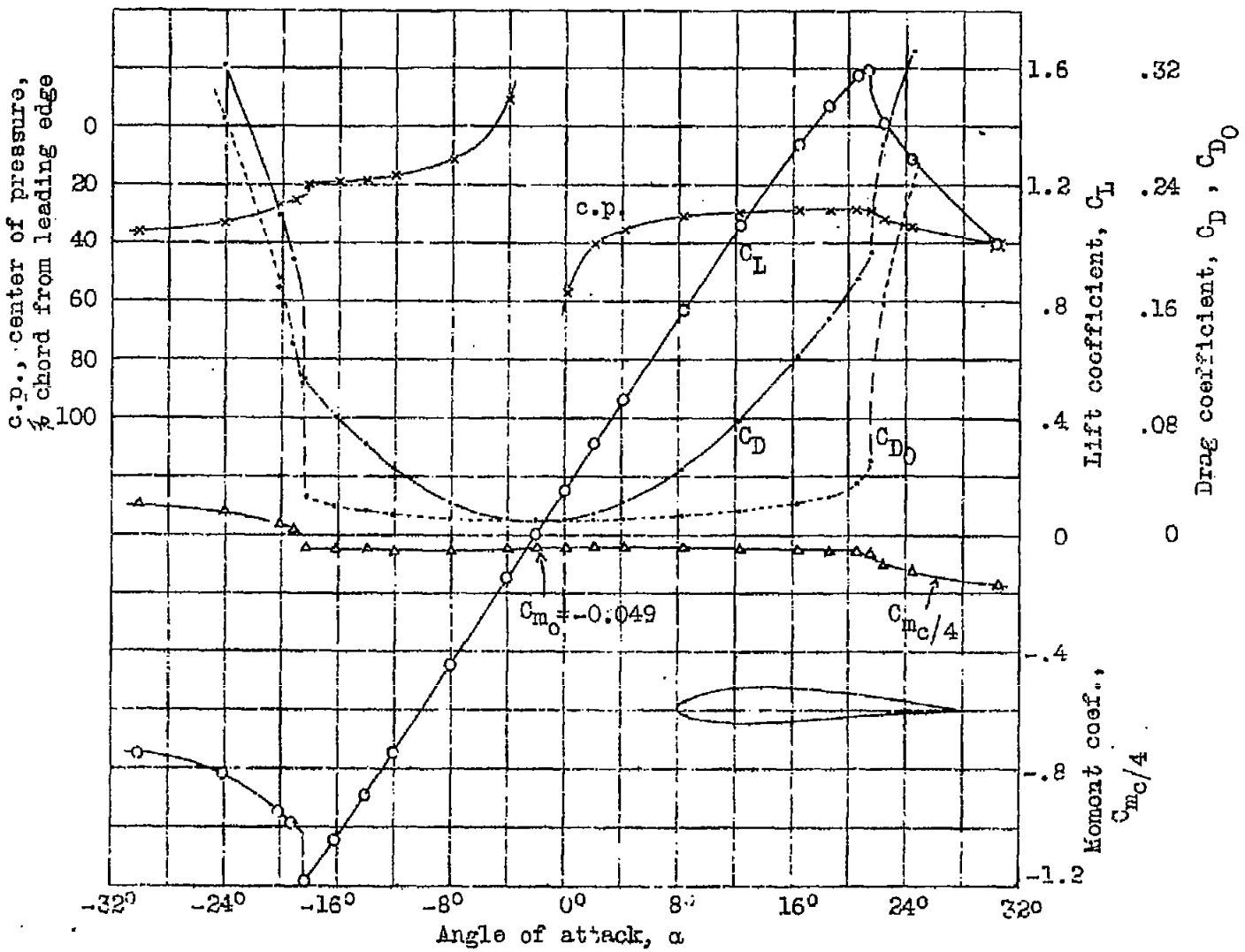

Fig. 23 Airfoil, N.A.C.A. 2512. Reynold's Number 7,100,000. V.D.T. tests, 674 and 648. Aspect ratio, 6. Tunnel wall correction applied. Dates, 9/31 and 8/31.

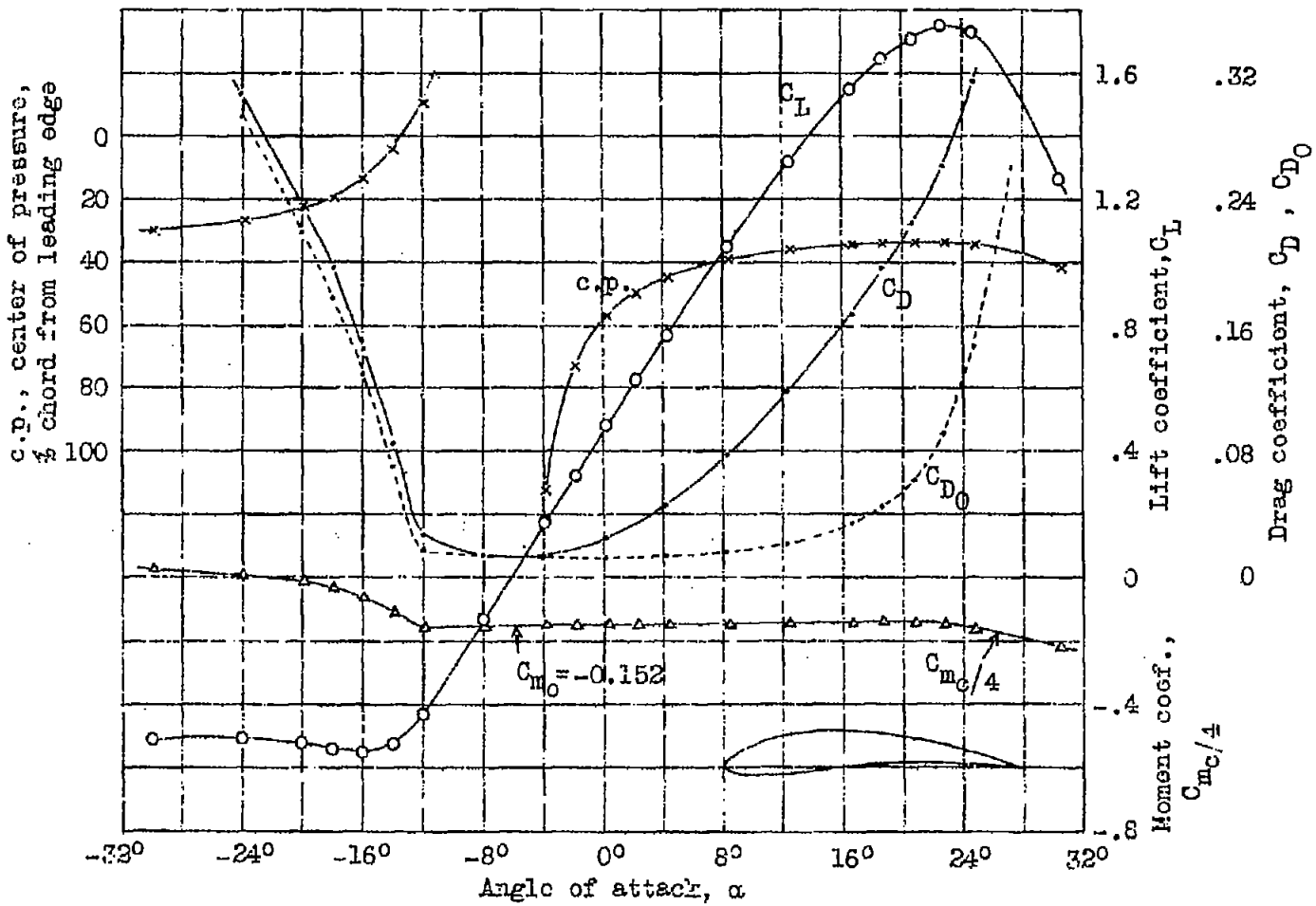

Fig. 24 Airfoil, N.A.C.A. 6512. Reynold's Number 3,100,000. V.D.T. tests, 584 and 647. Aspect ratio, 6. Tunnel wall correction applied. Dates, 4/31 and 8/31.

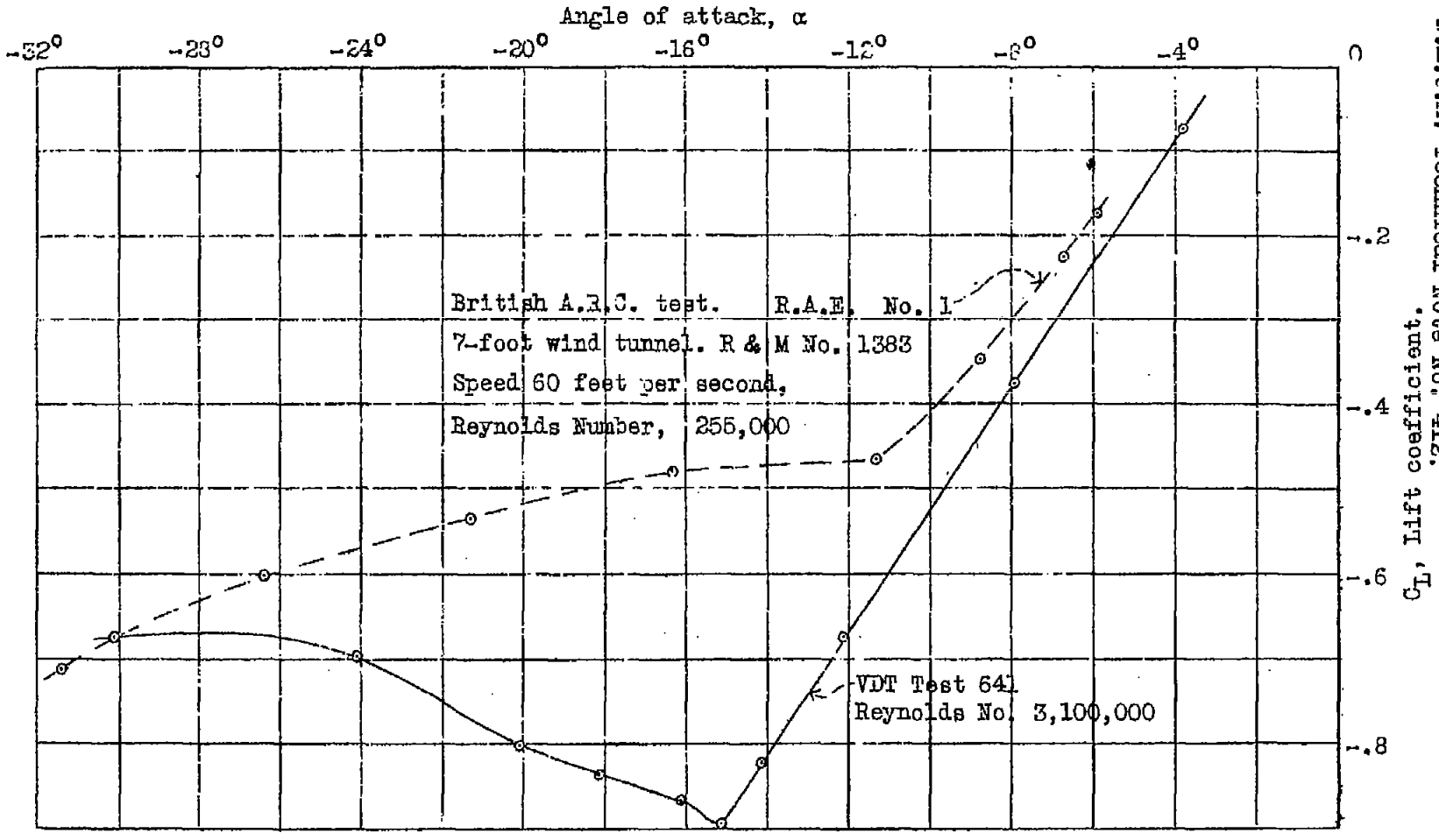

Fig. 25 Scale effect on the lift curve (negative range) of the CYH airfoil.

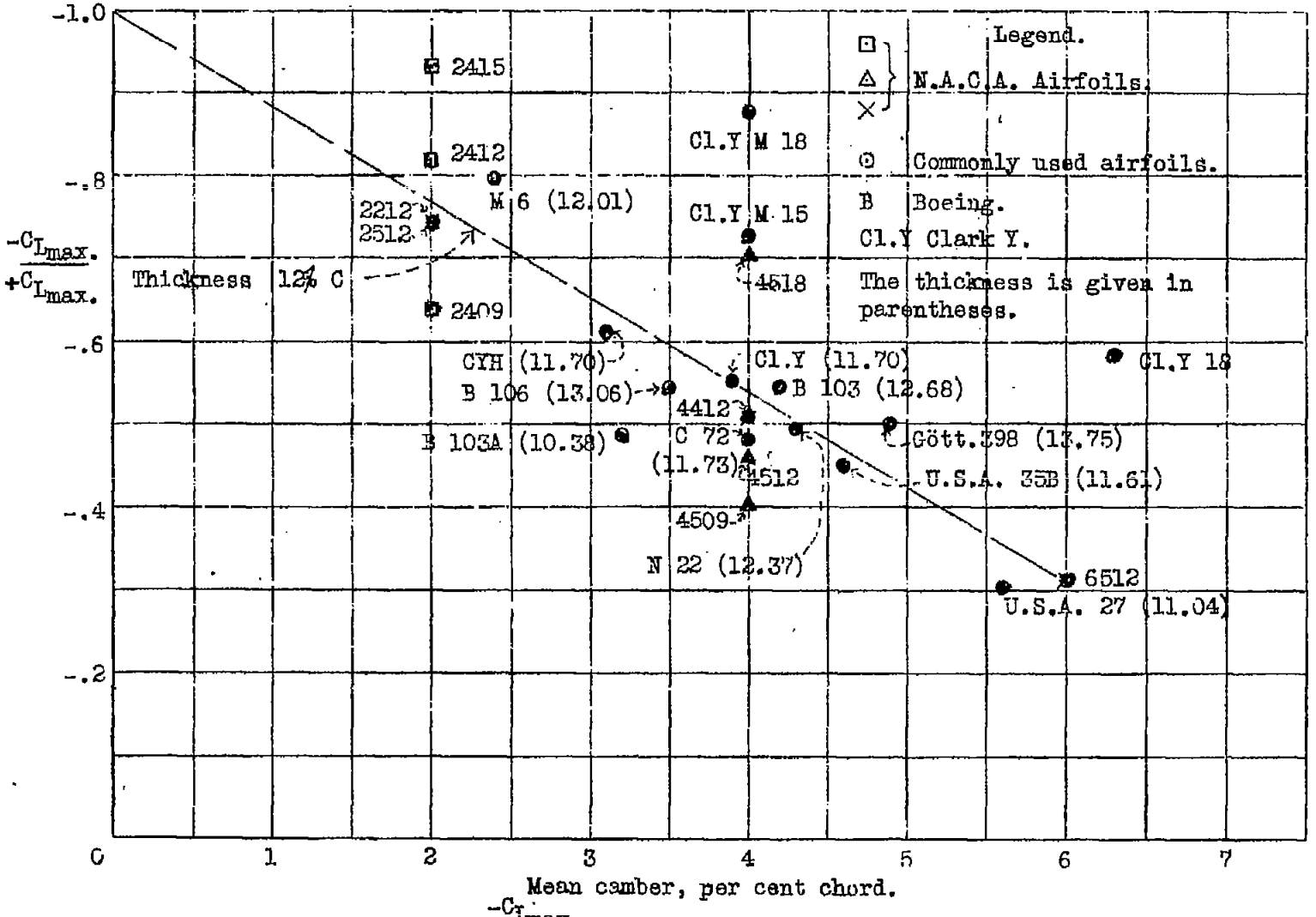

Fig. 26 Variation of $\frac{-C_{L_{max.}}}{+C_{L_{max.}}}$ with the mean camber and thickness of the profiles.